Open Ceramics 7 (2021) 100137

Contents lists available at ScienceDirect

Open Ceramics

journal homepage: www.editorialmanager.com/oceram

Sintering aids, their role and behaviour in the production of transparent ceramics

Jan Hostaša [a,*], Francesco Picelli [a,b], Soňa Hříbalová [c], Vojtěch Nečina [c]

[a] CNR ISTEC, Institute of Science and Technology for Ceramics, Italian National Research Council, Via Granarolo 64, 48018, Faenza, Italy
[b] Università Degli Studi di Parma, Via Università 12, Parma, PR, Italy
[c] Department of Glass and Ceramics, University of Chemistry and Technology, Prague (UCT Prague), Technická 5, 166 28, Prague 6, Czech Republic

ARTICLE INFO

Keywords:
Transparent ceramics
Sintering aid
Sintering

ABSTRACT

Transparent ceramics have been in the spotlight as advanced optical ceramic materials for the last two decades, both as optically transparent materials with excellent mechanical properties and with rare earth doping for applications in photonics, and even more so with the wider use of compact diode-pumped lasers. Sintering aids have been widely used in the production of a variety of transparent ceramics, removing porosity, enhancing the optical quality and providing a more uniform microstructure. This review aims to provide an overview of the state of the art and to point out both the most promising approaches and additives, as well as the important issues in the production of transparent ceramics and their properties related to the use of sintering aids, e.g. their incorporation in the ceramic crystal structure, the presence of secondary phase derived from sintering aids, or their double use as charge compensators.

1. Introduction

Traditionally, among inorganic materials, transparency has been the domain of glasses and single crystals, while the optical properties of ceramics have not been among the most important, apart from aesthetics. This changed in the 1960s when Coble developed translucent (in the title of his patent described as transparent, but, as was later written by Krell et al. [1], transparent materials should "provide clear images with a larger distance between the object and the transparent window", and this should be valid also with increasing thickness of the window, which was not the case) alumina ceramics for sodium discharge lamp envelopes and used a consistent scientific approach to identify the mechanisms and conditions leading to the full densification of the material.

Transparency of ceramics is highly influenced by light scattering on residual pores, inclusions of secondary phases or impurities and, in the case of birefringent materials, light scattering by randomly oriented birefringent grains. The reason behind light scattering is that these scatterers act as optical heterogeneities, i.e. there is a difference between refractive index of matrix (here ceramics) and the scatterer.

The impact of light scattering on transmittance is mainly influenced by the concentration of scatterers. The size of scatterers has also crucial effect that is additionally dependent on the wavelength of light. Similarly, both refractive indices of ceramics and scatterers are wavelength dependent. Moreover, simply said, the larger the difference between refractive indices of scatterers and matrix, the more light is scattered. If the scatterers are absorbing (e.g. carbon contamination or oxygen vacancies), the optical transparency further deteriorates. Light scattering by pores in transparent ceramics has been extensively studied by many authors (e.g. Refs. [1–7]), usually by predictions based on Mie theory or different approximations. A detailed description of methods for light scattering predictions is beyond the scope of this paper and therefore we refer to recent review paper on this topic [8].

The approach taken by Coble to eliminate the scatterers, mainly porosity, was to study combinations of different atmospheres and sintering aids, and their effect on the diffusion and densification of the material. Coble clearly stated that densification is limited when a non-diffusing gas atmosphere is trapped in the pores [9]. He identified the combination of MgO as a sintering aid and hydrogen atmosphere as a suitable method to eliminate gas from pores by increasing the sintering rate and suppressing discontinuous grain growth, in order to reach transparency. In later studies it has been shown that in the case of Al_2O_3 it is possible to produce fully dense ceramics even without the use of a sintering additive, and nearly transparent materials may be obtained when they have a very fine-grained microstructure [10,11]. The further problem with the full transparency of alumina is its non-cubic crystalline structure and the optical anisotropy leading to transmittance losses due

* Corresponding author.
E-mail address: jan.hostasa@istec.cnr.it (J. Hostaša).

https://doi.org/10.1016/j.oceram.2021.100137
Received 31 December 2020; Received in revised form 14 May 2021; Accepted 27 May 2021
Available online 8 June 2021
2666-5395/© 2021 The Author(s). Published by Elsevier Ltd on behalf of European Ceramic Society. This is an open access article under the CC BY license (http://creativecommons.org/licenses/by/4.0/).

to birefringence. In the case of non-cubic ceramics, there are differences in refractive index at grain boundaries caused by birefringent nature of the crystal and random orientation of grains. The problem of birefringent grains and their effect on the transmittance of ceramics has been also a point of interest for some authors [12,13], however, the models and calculations seem to be either incorrect or still have many shortcomings, as was recently explained by Pabst et al. [14].

After the first impulse and indication towards the fabrication of transparent ceramics given by Coble, a number of ceramics has been produced in translucent-to-transparent quality, e.g. transparent Y_2O_3 ceramics with LiF [15], or translucent yttrium aluminium garnet (YAG) ceramics prepared from YAG powders by vacuum sintering with the addition of MgO and SiO_2 as sintering aids [16]. By the end of 1980s, however, the optical quality of transparent ceramic was limited. The situation changed completely in the 1990s thanks to the effort of two research groups in Japan: that of Haneda involving the Konoshima Chemical Co. [17] and the research group of Akio Ikesue [18], both presenting unprecedented results in the fabrication of transparent ceramic Nd-doped[1] yttrium aluminium garnet, Nd:YAG, with quality close to that of single crystals. In both cases the authors used SiO_2 as the sintering aid, in the former introduced as colloidal silica, in the latter as tetraethyl orthosilicate, TEOS, the organic precursor of SiO_2. The two pioneering groups have since remained leaders in the development and production of high-quality transparent ceramics. In the following decades, the research on transparent ceramics has been extensive [19–23], and materials of high optical quality were obtained, often with the use of sintering aids. Some transparent ceramics may be prepared without the use of a sintering aid (e.g. $MgAl_2O_4$ spinel [24], Al_2O_3 [25,26], CaF_2 [27], $(La,Y)_2O_3$ [28]), often thanks to a combination of suitable starting powders and a densification process providing a significant driving force to the sintering process, viz. Hot Isostatic Pressing (HIP) or Spark Plasma Sintering (SPS). Nevertheless, the use of sintering aids and its optimisation have been of major interest in the last four decades.

Nowadays, transparent ceramic materials are a valid group of materials with different applications, albeit with a limited commercialisation yet. One of the key elements of the production process is the use of sintering aids. While there is a consensus on their use in general, backed by empirical evidence, some aspects are still not clear or sufficiently described. In the present work we aim to provide an overview of the state of the art and to point out both the most promising approaches and the potentially missing pieces of the puzzle.

2. Sintering aids

The main issues addressed in the process planning in order to eliminate porosity are the selection of highly pure starting powders with high sinterability and suitable particle size [1], good particle packing in the green body and a sintering step that leads to the densification without exaggerated grain growth, which could lead to the closure of pores inside grains.

Sintering aids usually help with the reduction of sintering temperature and with the elimination of pores from ceramic materials either through the presence of a liquid phase, or by other mechanisms that support the densification of ceramics, e.g. by introducing dislocations and enhancing diffusion during thermal treatments. Sintering is mostly accompanied by grain growth, as the reduction of the grain surface (grain boundaries) is energetically favourable. When the grain boundary mobility is too high, pores remain trapped inside the fast growing grains, and are then difficult (nearly impossible) to eliminate, as the diffusion of the gas entrapped inside pores is faster along grain boundaries compared to the grains. In comparison with other types of ceramics, in transparent ceramics it is crucial that no secondary phase remains at the grain boundary of the sintered material. The difference of the refractive index of the crystalline grains and the secondary phase would lead to the scattering of light and thus to losses in the in-line transmission. The additives therefore need to either leave the material during the sintering step, or dissolve into a solid solution with the ceramic matrix. For the consideration of the latter it is thus very useful to know the solubility limit of the different ions in the ceramic [29]. The additives should also not introduce any defect states in the band gap of the ceramics [30].

The most commonly used sintering aids are oxides SiO_2 (added in the form of silica powder, colloidal silica or the organic precursor TEOS – tetraethyl orthosilicate), MgO, CaO, etc. or alkali halides, above all LiF. Other additives mentioned to a lesser amount in the literature are ZrO_2, La_2O_3, B_2O_3 or Sc_2O_3. Eventually, the sintering aids can also be combined, as the different aids use different mechanisms to promote densification and the removal of pores.

2.1. SiO_2

SiO_2, often added in the form of TEOS, has been used largely for the sintering of transparent garnet ceramics by vacuum sintering, above all for the production of transparent YAG. The addition of SiO_2 promotes densification, elimination of pores and grain growth [31], as is illustrated in Fig. 1 for YAG, Nd:YAG and Yb:YAG. The grain growth may become problematic for the complete elimination of porosity when some pores remain entrapped within larger grains, as pointed out also by Boulesteix et al. [32].

While the beneficial effect of SiO_2 on the densification and closure of pores was recognized after empirical results [18,36,37], the sintering mechanism of YAG ceramics with SiO_2 has been widely discussed in the literature in past two decades, and still requires further analysis. Boulesteix et al. proposed a liquid phase sintering model for Nd:YAG after they observed a significant increase in densification rate and found intragranular inclusions of silica after vacuum sintering with a relatively high amount of SiO_2 (0.3 wt%) [32,38,39]. However, when using 0.14 wt % of SiO_2 (equivalent to 0.5 wt% of TEOS), other authors did not observe any amorphous phase at the grain boundaries [3,40], which would support the liquid phase model, except for sample prepared with a very low cooling rate [3]. Stevenson et al., on the other hand, proposed that a solid solution is formed with Si^{4+} ions substituting Al^{3+} ions in the tetrahedral site of the YAG crystal structure, as supported by NMR analysis, and the densification follows a solid state mechanism via solute drag effect [35]. This is consistent with *ab intio* simulations [30]. In a later study, Boulesteix et al. [41] discussed the effect of the amount of SiO_2 on the sintering mechanism of Nd:YAG. The authors sustain the liquid phase sintering mechanism for elevated additions (0.3 wt% of SiO_2, about double the usually used amount), while for lower additions, below the Si solubility limit in YAG, they agree on the solid-solution hypothesis, which would enhance the diffusion kinetics. Moreover, they report on the decrease of Si content in YAG at advanced stages of the vacuum sintering process, an observation later confirmed by LIBS studies [42,43]. This decrease would be due to the evaporation of volatile SiO at higher temperature. More recently, Goldstein et al. considered the lattice distortion due to the substitution of larger Al^{3+} ions (0.39 Å) by smaller Si^{4+} (0.26 Å) in the YAG crystal structure to be the driving mechanism of the diffusion and sintering of the ceramics, furthermore, helping with the incorporation of larger rare earth ions. In the case of rare earth ions larger than Y^{3+}, grain boundary segregation was observed and in the case of Stevenson [35] attributed to the solute drag effect.

It is important to note that the segregation of rare earth dopant on the grain boundaries depends on the dopant itself and on the difference between the dopant ion size and that of the substituted ion, here Y^{3+}. While in the case of relatively large ions like Nd^{3+} [44] or Ce^{3+} [45] grain boundary segregation has been observed, in the case of Yb^{3+} (ionic radius comparable to that of Y^{3+}), this was not the case [46], although in both cases SiO_2 was used as the sintering aid. Some Si enrichment at

[1] Throughout this article we distinguish between the *dopants*, ions providing functionality, and often changing the spectroscopic properties, and *sintering aids*, which serve to enhance densification of the ceramic.

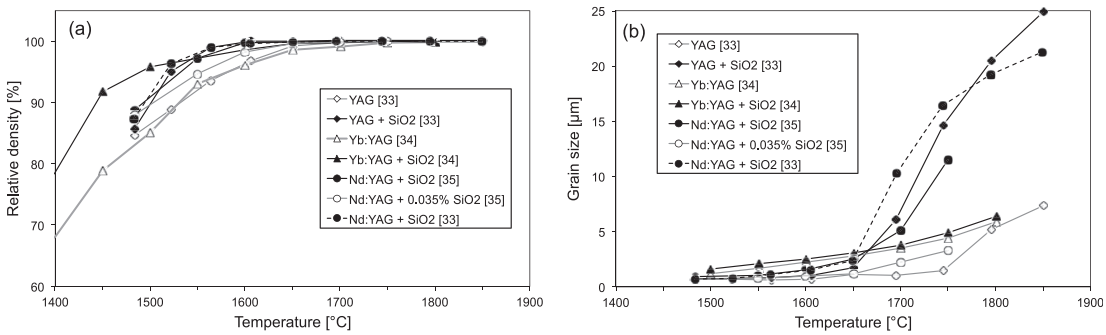

Fig. 1. Relative density (a) and grain size (b) as a function of vacuum sintering temperature (2 h dwell time at each temperature); data taken from Refs. [33–35], all the SiO_2 additions were 0.14 wt% (0.5 wt% of TEOS), except for the "Nd:YAG + 0.035% SiO2", which represents a low Si concentration counterpart.

grain boundaries has been observed in YAG and Yb:YAG ceramics [47,48]. As mentioned above, an important parameter influencing the final microstructure and the presence of secondary phases at grain boundaries is the cooling rate and the solubility of Si in YAG [3,29]. This is further discussed in section 4.

The amount of SiO_2 typically used to produce YAG ceramics by vacuum sintering is 0.14 wt%, corresponding to 0.5 wt% of TEOS. The effect of the decrease of SiO_2 addition from 0.14 wt% to 0.085 wt% (0.5 wt% TEOS to 0.3 wt%) has been studied by Hostaša et al. [49], showing a decrease in optical quality with the reduction of the SiO_2 amount. The authors suggest that longer sintering times could compensate the transparency losses. The effect of SiO_2 amount on the sintering of YAG is illustrated in Fig. 2; the SEM micrographs show the elimination of porosity and the grain growth connected to higher additions, and the optical quality of the ceramics is shown in the photographs. In the case of 1 wt% TEOS (equivalent to 0.28 wt% of SiO_2), the grain growth is significant and some pores are already entrapped inside grains.

When vacuum sintering was coupled with a HIP post-treatment, transparent ceramics could be also obtained with 0.14 wt% SiO_2 [50], the amount of SiO_2 could be significantly reduced (to 0.02 wt%), as illustrated by Lee et al. for Nd:YAG [40]. Recently, Ikesue et al. [51] prepared Yb:YAG without the use of sintering aids by vacuum sintering coupled with HIP, while later Chen et al. [52] managed the task by vacuum sintering only.

Apart from YAG, SiO_2 proved useful also in the vacuum sintering or vacuum sintering + HIP treatment of other garnets. Yb:LuAG (lutetium aluminium garnet) ceramics have also been prepared by reaction

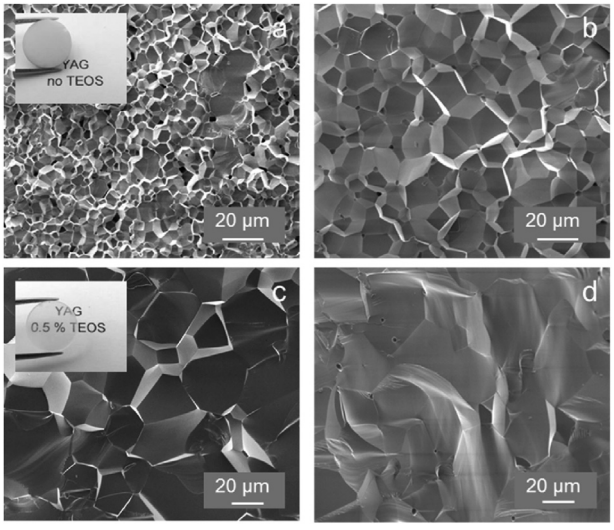

Fig. 2. Fracture surface seen by SEM of YAG ceramic samples obtained with an initial addition of 0 (a), 0.25 (b), 0.5 (c) and 1 wt% (d) of TEOS, and in the insets photographs of the respective samples with 0 (a) and 0.5 wt% (c) of TEOS. Source [43].

sintering under vacuum with the addition of 0.07–0.28 wt% of SiO_2 introduced in the form of TEOS [53]. According to the authors, the Si solubility limit appears to be much lower compared to that in YAG, only 0.07 wt% of SiO_2. Interestingly, there was not a significant grain growth associated with the addition of SiO_2, none when the amount of SiO_2 was increased from 0.07 to 0.28 wt%. The authors assumed this to be the effect of a liquid phase present at grain boundaries, however they did not show or mention any secondary phases at grain boundaries in the samples with higher Si content, while a change in the lattice constant of the material kept changing up to the addition of 0.14 wt% of SiO_2. It is thus likely that although the optimal addition of SiO_2 for achieving transparency is close to 0.07 wt%, the solubility limit is higher. Nd:LuAG and Nd:YSAG (yttrium scandium aluminium garnet) can be prepared with 0.1 wt% of SiO_2 [54]. Ce:GGAG (gallium gadolinium aluminium garnet) was prepared by sintering in air followed by HIP with 0.14 wt% SiO_2 [55]. In the case of TAG/TYAG (terbium aluminium garnet/terbium yttrium aluminium garnet) ceramics, Aung and Ikesue managed to prepare nearly perfect material using only 0.01 wt% of colloidal silica and the combined vacuum sintering and post-HIP treatment. When a higher amount of SiO_2 was used, Al_2O_3 inclusions could be observed in the microstructure, unless a longer pre-sintering times were used [56].

2.2. MgO

MgO has been successfully proposed as the suitable sintering aid for translucent Al_2O_3 ceramics by Coble [57], with its presence inhibiting exaggerated grain growth by the solute drag mechanism [58]. MgO proved useful also for vacuum sintering when added in the amount of 0.05–0.25 wt% [59]. Nevertheless, due to the birefringence of the material, the achievement of transparency of Al_2O_3 is guided prevalently by the use of fine starting powders and a pressure-assisted sintering technique.

MgO can be used as a sintering aid in YAG ceramics, where Mg^{2+} will preferentially substitute Al^{3+} in the octahedral site [30]. As in the case of Al_2O_3, also in YAG MgO inhibits grain growth, by the solute drag mechanism; the reduced grain size in comparison to YAG with SiO_2 has been observed even at high sintering temperatures [60]. This is in accordance with the observations on grain boundary mobility in Mg^{2+}-containing YAG, about one order of magnitude lower compared to YAG with Si^{4+} [61]. The limitation of grain growth likely derives from the presence of Mg at grain boundaries at intermediate sintering temperatures, while the Mg^{2+} substitution for Al^{3+} in the octahedral site of YAG and the thus derived oxygen vacancies enhance the sintering process. This principle is used to stabilize Cr^{4+} ions in Cr:YAG, as described in the following section. However, Doroshenko et al. [62] suggest that at high sintering temperatures (above 1750 °C) Mg^{2+} may occupy interstitial position in YAG, and the stabilisation efficiency will decrease. Compared to SiO_2, the useful amount of MgO in YAG is significantly lower, as is also its solubility in the YAG matrix (0.14 wt% SiO_2 vs. 0.06 wt% MgO [29,63]).

The use of divalent sintering aids like MgO and CaO in YAG has to be approached with care when it comes to annealing in air, which is sometimes necessary for the removal of oxygen vacancies or reoxidation of dopants after vacuum sintering. It has been observed that after annealing at elevated temperatures (1450 °C for 10 h), colour centres were formed, deriving from Mg^{2+} and Ca^{2+} [64]. An opposite situation is the case of vacuum-sintered Eu:YAG [65]. Here, the addition of TEOS causes the presence of a series of absorption bands originating from colour centres, in particular the $Eu_Y^{2+} + F^+$ pair, that has been observed to form easily in the presence of Si^{4+} ions. These absorption bands are not observed when MgO is used as a sintering aid.

Similarly to YAG, also LuAG ceramics can be sintered under vacuum to transparency with the use of MgO. In Ce:LuAG the addition of MgO not only improved transparency by the elimination of Al-rich secondary phases, but also the scintillation performance [66]. The addition of only 0.02 wt% MgO in Cr,Nd:LuAG was sufficient to provide transparent ceramics sintered by the combination of vacuum sintering and HIP [67]. In Pr:LuAG, the use of 0.01 wt% of MgO allowed to significantly reduce the annealing temperature [68]. This effect is due to charge compensation, discussed in the following section.

2.3. $MgO + SiO_2$

The combination of MgO and SiO_2 is very promising for the vacuum sintering of YAG ceramics [69–72], because while SiO_2 effectively eliminates porosity, the addition of MgO limits grain size, allowing a better densification potentially even in larger volumes of material. The amount of MgO is usually lower than that of SiO_2. Liu et al. used 0.01 wt % MgO with 0.14 wt% SiO_2 to obtain Nd:YAG by vacuum sintering [73], but observed residual inclusions of $MgAl_2O_4$ already when the MgO amount was increased to 0.012 wt%.

Another advantage of the mixture of SiO_2 and MgO is in the elimination of colour centres deriving from Mg^{2+} [34]. *Ab initio* simulations suggest that MgO and SiO_2 would form a liquid phase, enhancing the densification rate [30]. While the aim of this article is to discuss sintering aids in relation to densification, it is worth mentioning that as any additive, also sintering aids may influence other process parameters, e.g. the rheological properties of slurries for casting processes [71].

In Pr:LuAG the use of 0.2 wt% of TEOS and 0.2 wt% MgO enhanced the optical quality but a deleterious effect was observed on the scintillation properties due to the formation of point defects [74].

An extensive research has been dedicated also to the use of the mixture of SiO_2 and MgO in the production of TAG ($Tb_3Al_5O_{12}$) magneto-optical ceramics, which are particularly difficult to obtain as single crystals due to incongruent melting. The optimal amounts used for vacuum sintering were 0.4 wt% TEOS (~0.11 wt% SiO_2) and 0.1 wt% MgO [75,76]. Chen et al. [75] observed a slight decrease of optimal sintering temperature with the increase of MgO content (1670 °C–1640 °C), while the grain growth was inhibited for small additions of MgO (from 0 to 0.06 wt% the mean grain size changed from about 23 to 11 μm, respectively) and increased steadily with higher MgO content (for 0.2 wt % of MgO the authors reported more than 30 μm mean grain size). A small increase of SiO_2 content on the other hand improved the optical transmittance and the presence of Si^{4+} ions substituting Al^{3+} in the garnet structure is advantageous by preventing the transition of Tb^{3+} to the undesired Tb^{4+} state [76]. In both [75,76] the authors assume the presence of liquid phases during the sintering process, but they do not provide relevant data to support the claim. The combination of vacuum and HIP was also used for TAG, with the optimum amounts being 0.4 wt % of TEOS and 0.1 wt% of MgO, and with MgO inhibiting grain growth [77].

2.4. CaO

CaO also effectively inhibits grain growth when used in YAG ceramics sintered under vacuum. Hua et al. [78] studied the effect of different amounts of CaO in YAG sintered at 1780 °C for 20 h under vacuum, and demonstrated that additions of 0.1, 0.3 and 0.5 at.% of CaO result in higher transmittances than YAG without any sintering aid (at least at wavelengths larger than 400 nm), while higher concentrations (0.7 and 1.0 at.%) led to transmittances even lower. In general, the most suitable concentration of CaO seems to be the lowest one, 0.1 at.%. It was also shown that at low CaO concentrations, the grain growth is inhibited, whereas when the concentration of CaO is higher than 0.3 at.% (0.085 wt %), the grain size increases and with even higher concentrations, grain boundary phases and large pores leading to significant decrease of transparency occur. Even after a sintering step performed at elevated temperatures (up to 1820 °C, compared to the generally used range of 1700–1750 °C), the fine-grained structure was reported to maintain the mean grain size below 3 μm after the addition of 0.045 wt% of CaO [79]. The mean grain size of vacuum-sintered YAG with SiO_2 can be larger by a factor of ten.

2.5. $CaO + MgO$

Zhou et al. [80] studied the optimal ratio of CaO to MgO for achieving highest optical quality in undoped vacuum-sintered YAG and found out, that 1:4 M ratio is ideal (in all of the cases total 0.2 mol% of CaO and MgO according to Al^{3+} content was added). Using only CaO led to the smallest grain sizes for all sintering temperatures (different sintering temperatures between 1540 and 1780 °C for 8 h in vacuum), whereas the use of MgO only led to largest grain sizes in samples with sintering aids (also for all sintering temperatures). Grain sizes achieved by addition of different ratios Ca:Mg were found to be between grain sizes of samples with only CaO and MgO. Therefore, it can be concluded that the higher amount of CaO with respect to MgO, the smaller grain sizes can be achieved. Nevertheless, the highest transparency was attained with molar ratio Ca:Mg = 1:4 closely followed by Ca:Mg = 2:3. Addition of only CaO led to the worst transparency, while addition of MgO led to better, yet among other samples mediocre transmittances.

This is in agreement with results reported by Chaika et al. [81], who presented similar transmittance results for ceramics with 0.15 at.% MgO. Addition of 0.5 at.% MgO, however, leads to significant decrease in transmittance, while addition of 0.05 at.% MgO results only in slight, approximately 5% drop compared to the sample with 0.15 at.% MgO. We can thus assume, that amounts of MgO lower than 0.15 at.% (down to 0.05 at.%) have little effect on transparency, whereas higher amounts have a significantly negative impact.

It was also reported in another paper by Chaika et al. [82], that the addition of CaO results in fully opaque samples due to large amount of residual porosity. While Zhou et al. [80] was able to achieve some level of transparency using CaO, it was still the worst among all of the samples with different ratios of Ca:Mg, including only Ca and only Mg. However, in a more recent publication by Chaika et al. [64], transparent samples of Cr:YAG with CaO as sintering aid (and simultaneously charge compensator) were presented. The dependence of Ca amount on transparency is highly non-linear and highest transmittance was achieved by using 0.5 at.% Ca. Zero transmittance was measured in sample with 0.16 at.% of Ca and was caused by pores with size around 1 μm. The transparency and microstructure are said to be outcome of interaction between CaO and Cr_2O_3 resulting in presence of liquid phase on grain boundaries.

Chaika et al. [64] assume that while MgO and Cr_2O_3 do not interact during the sintering process, the combination of CaO and Cr_2O_3 does, improving the optical quality in comparison with a dopant-free YAG with CaO as sintering aid. The authors of this paper hope that further research will shed more light on the possible combination of CaO with dopants in garnet ceramics.

Grain sizes reported by Chaika et al. seem to be in agreement with Zhou et al. as well. Additionally, Chaika et al. showed that the grain size for the lowest amount of Ca (0.16 at.%) is the smallest and increases with Ca amount.

2.6. La_2O_3

Among sesquioxides, La_2O_3 is the one most commonly used as a sintering aid. Typically it is added to other sesquioxides, e.g. Y_2O_3 [83], and since the amount can be even 10 mol.%, it may be questionable, if it is a typical sintering aid, or whether the obtained material is not simply a mixed sesquioxide. Such systems can have a lower melting, and also sintering temperature. Nevertheless, La_2O_3 is potentially a useful sintering aid for Y_2O_3 (1.57 mol.% addition), promoting densification at temperatures above 1550 °C [84], or combined with ZrO_2 to limit the grain growth.

La_2O_3 has been also reported as an additional sintering aid to TEOS in Nd:YAG ceramics, where its role was the limitation of grain growth, with optimum addition of 0.8 wt% [85], and a slight decrease of the required sintering temperature compared to the use of SiO_2 only [86]. Higher amounts of La_2O_3 then led to the segregation of secondary phases on grain boundaries.

Stuer et al. showed that La_2O_3 can be also used as an efficient sintering aid for polycrystalline Al_2O_3 ceramics, and the best results were obtained when MgO and Y_2O_3 were also introduced [10].

2.7. Sc_2O_3

The combination of Sc_2O_3 and La_2O_3 in vacuum-sintered Pr:YAG provided good optical transmittance and a microstructure with finer grains compared to the combination SiO_2–MgO. However, a higher concentration of La_2O_3 and Sc_2O_3 led to the deterioration of scintillation efficiency [87]. When used together with SiO_2 in Yb:LuAG, the addition of Sc_2O_3 improved the optical quality after HIP treatment [88].

2.8. B_2O_3

While the use of B_2O_3 alone has not been particularly endorsed, it has provided very promising results when combined with SiO_2 in vacuum-sintered YAG ceramic, in particular in the case of reactive sintering, YAG phase formed at lower temperature [89]. The advantage of B_2O_3 as a sintering aid is its evaporation at elevated temperatures (above 1500 °C), and the reduction of the sintering temperature by ~100 °C.

B_2O_3 has also been used as a sintering aid (addition of 0.15 wt%) in spinel ceramics obtained by HIP, both reducing the sintering temperature and inhibiting grain growth [90].

2.9. ZrO_2

ZrO_2 finds use in the vacuum sintering of sesquioxides, in particular of Y_2O_3. As vacuum sintering promotes the formation of oxygen vacancies in the material, leading to darkening and to the deterioration of optical properties. Interestingly, to enhance the oxygen stabilisation without introducing too much of the sintering aid, Jung et al. [91] proposed the sintering of the Y_2O_3 ceramic pellet in an Y_2O_3 powder bed surrounded by ZrO_2 powder. This approach uses ZrO_2 to prevent the formation of oxygen vacancies, while limiting the necessary amount of the aid in the material itself. 3 mol. % of ZrO_2 were added to the Y_2O_3 powder. In Tm:Y_2O_3–La_2O_3 ceramics, ZrO_2 (3 at.% Zr with respect to Y) was successfully used to limit grain growth and promote transparency [84], and the combination of 1.6 wt% ZrO_2 and 0.1 wt% MgO led to very high transparency in vacuum sintered Yb:Y_2O_3 [92].

In Nd:YAG, the simultaneous use of ZrO_2 and SiO_2 enhances diffusion rate and limits grain growth. The latter can be expected given the significantly lower grain boundary mobility in YAG with Zr^{4+} (6.7×10^{-16} $m^3N^{-1}s^{-1}$) compared to YAG with Si^{4+} (2.0×10^{-14} $m^3N^{-1}s^{-1}$) [61]. However, when sintered at too high temperature (1800 °C), the combined effect of ZrO_2 and SiO_2 leads to the segregation of Al_2O_3 at grain boundaries due to the possible substitution of Al^{3+} ions in YAG by both Si^{4+} and Zr^{4+} ions [93].

2.10. LiF, fluorides

While the use of SiO_2, MgO and CaO is most common in vacuum sintering, LiF and other halides on the other hand are used in pressure-assisted sintering methods, viz. hot pressing (HP) and spark plasma sintering (SPS). Both HP and SPS mostly use graphite equipment (molds, pistons), which may cause carbon contamination of the ceramic material [94–96] and, consequently, a deterioration of optical properties due to scattering and absorption. Apart from enhancing the densification, the use of halides can also prevent this contamination.

2.11. LiF

LiF melts at about 850 °C [19] and creates a low-viscosity lubricating film on the particles, allowing them to slide and rearrange and leading thus to a better densification through the liquid-phase sintering. With increasing temperature, LiF evaporates and leaves the material before the pore closure. LiF is the additive of choice in the densification methods involving uniaxial pressure, e.g. hot pressing (HP) and spark plasma sintering (SPS).

Among transparent ceramic materials, LiF has been most known and most widely used in the production of $MgAl_2O_4$ spinel. There has been a massive interest in the production of transparent spinel ceramics due to its high theoretical transparency, low density, good mechanical properties and thermal, chemical and mechanical resistance. As summarized in the comprehensive review by Rubat du Merac et al. [97], a wide range of sintering additives has been tested for the production of transparent spinel ceramics, including both oxides, halides, and their combinations, e.g. CaO [98], B_2O_3 [90], TiO_2, LiF [99–103], LiF + $CaCO_3$ [104]. Eventually, LiF has been the additive providing the best results, in particular for pressure-assisted sintering methods.

Apart from the low viscosity of the liquid film, another advantage of LiF is the very good wetting of the spinel system [105] which allows for its homogeneous dispersion on the surface of the particles. In the case of reactive sintering, the addition of LiF promotes the formation of the spinel phase [104,106]. Moreover, the presence of LiF film prevents the penetration of carbon inside the material. While the effect has been observed by many authors, there is not a consensus regarding the mechanism behind it [100,106–108]. Goldstein [100] suggests that after the liquid-assisted-sintering in the temperature range between 850 °C and 1300 °C LiF does not react with spinel, but seals the material, preventing thus the contamination with carbon. When LiF eventually evaporates, the material is already dense enough to withstand the penetration. Esposito et al. [106] took a similar view, concluding that the liquid phase covering the grains prevents carbon contamination.

The mechanism of interaction between LiF and spinel is still a matter of discussion, as there is still a lack of evidence to fully support a single model. Reimanis and Kleebe [109] proposed a hypothesis assuming that the evaporation of LiF leads to the reprecipitation of dissolved spinel, where Li^+ and F^- ions are incorporated in the spinel matrix, substituting Mg^{2+}, Al^{3+} and O^{2-}, respectively. This substitution would thus lead to the creation of oxygen vacancies, which decrease the activation energy of sintering, thus lowering the sintering temperature. Later, Goldstein et al. [100] rightly pointed out that substitution of Al^{3+} by Li^+ is very unlikely due to relatively large difference in ionic radii and valence. Only Mg^{2+} would thus be substituted and no oxygen vacancies generated. Recently, Nečina and Pabst [107] agreed with Goldstein et al. in the former point, but assumed that oxygen vacancies are still created, lowering the activation energy of sintering. The authors adapted the hypothesis of Reimanis and Kleebe [109] and suggested that LiF behaves similarly to MgO in context of spinel, so if LiF substitutes MgO, the MgO is then dissolved in spinel resulting in a *pseudo-excess* of MgO. It is known that excess of MgO in spinel is compensated by oxygen vacancies [110].

With increasing temperature LiF eventually evaporates, unless trapped in the material, e.g. by the application of external pressure [111]. Indeed, the identification of the intermediate soaking step is one of the

crucial parameters for process optimisation. The final microstructure depends on the sintering method: materials produced by HP have usually larger grains compared to those obtained by SPS or by HIP. The optimal LiF addition is generally reported between 0.25 and 1.5 wt%, typically 1 wt% with respect to the dry ceramic powder [97,100–102,106,107,112,113].

Transparent Y_2O_3 was also obtained by HP with 1 wt% LiF [114], and with the wider use of SPS, LiF has been used to produce also transparent YAG [111,115], Dy:Y_2O_3 with 0.3 wt% LiF [116], Sm:Y_2O_3 [117], Nd:Lu2O3 [118] or MgO [119]. The LiF amount ranged from 0.2 to 1 wt %. In the case of YAG prepared by SPS, Katz et al. [111] pointed out that the starting powders should have as low sulphur content as possible to avoid the formation of S-rich phases arising from the reaction with LiF.

2.12. Other halides

When different alkali halides (LiCl, NaF, NaCl, KF, KCl) were tested as sintering aids for $MgAl_2O_4$ spinel ceramics produced by SPS [107], LiF provided the highest optical transmittance among the tested aids, while also causing excessive grain growth, which – as was confirmed – is caused by Li^+ ions, because similar grain size was observed in the case of LiCl (although with only a limited effect on densification). The authors observed decrease in the onset temperature of sintering down to 812 and 831 °C for LiF and NaF, respectively (compared to 989 °C for spinel without any sintering aid). The effect of the addition of LiF and NaF on SPS-produced $MgAl_2O_4$ spinel is illustrated in Fig. 3. The best optical quality is observed for LiF addition; in the case of spinel without additives, a dark coloration can be observed, which is mainly caused by the penetration of carbon into the ceramics during the sintering process. Both LiF and NaF prevented this effect, although the optical quality of samples with NaF was scarce. Moreover, NaF led to significant grain growth inhibition. Grain growth inhibition has been also observed in HP-produced spinel with the addition of MgF_2 [100]. The advantage of MgF_2 in spinel ceramics is the presence of Mg, which is already in the crystal lattice; for the same reason also $AlCl_3$ is a potential candidate [120].

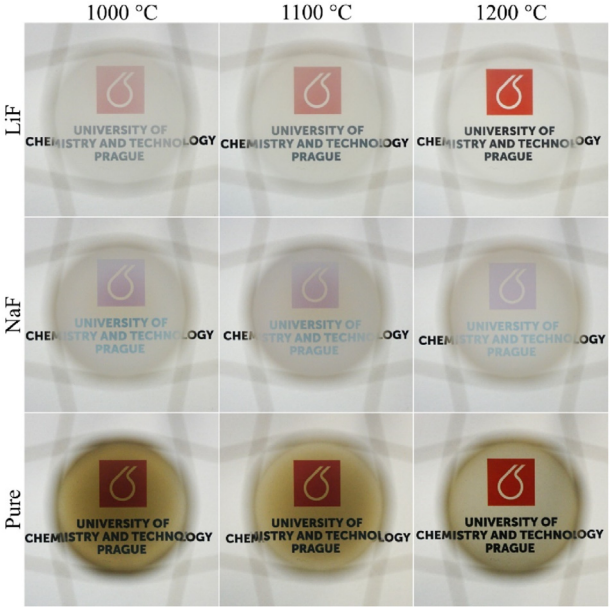

Fig. 3. View through spinel ceramic samples prepared by SPS with LiF (top row), NaF (middle row) and without sintering additive (bottom row), at 1000 °C (left column), 1100 °C (middle column) and 1200 °C (right column) as the temperature of first dwell; thicknesses of samples vary between 0.94 and 2.09 mm; samples are fixed in a wire frame in a distance approximately 10 cm above the logo in order to demonstrate the degree of in-line transmittance.
Source [107].

The volatility of fluorides makes them interesting for the possible limitation of the presence of sintering aid-based secondary phases. This approach has been tested for YAG with 0.57 wt% of the mixture of AlF_3 and YF_3 added together with a small amount (0.027 wt%) of SiO_2. The obtained results were promising, although some F impurities were observed in the sintered materials [121].

To provide also the perspective of materials selection, Table 1 shows a list of different transparent ceramics and the main sintering aids and processes used in their production. We chose not to include the different doping ions, so as to provide a more general overview. However, in some cases, the selection of the dopant or application dictates the sintering aid to be used. Probably the most specific case are dopants requiring charge compensation.

Unlike the addition of other sintering aids, where the optimal amount of sintering aid usually does not change much with functional doping, the charge compensation requires a balance between the amount of dopant and that of the sintering aid.

3. Charge compensators

Apart from the above described effect on the elimination of pores, the additives can have yet another role related mostly to the functional dopants in the transparent ceramics, that of a charge compensator. The dopants of interest have been above all Cr^{4+} and Ce^{4+} in garnet ceramics for the use as absorbers in the former, and scintillators and phosphors in the latter case. Here the dopants replace the ions in the dodecahedral sites (Y^{3+} in YAG, Lu^{3+} in LuAG, etc.), but after a vacuum sintering the ions are mostly present in the reduced form.

Therefore, the main challenge besides achieving high transparency in the preparation of Cr^{4+}:YAG ceramics is the conversion of chromium to its tetravalent state. That can be achieved by the addition of CaO and MgO as the charge compensators and sintering aids, and annealing after sintering [81,128]. SiO_2, commonly used in YAG is not suitable for Cr^{4+}:YAG, because Si^{4+} ions may occupy tetrahedral Al^{3+} positions in the lattice and that due to the $^{4+}$ charge inhibits the conversion efficiency of Cr^{2+} and Cr^{3+} ions to Cr^{4+} [129]. In general, it was found that the addition of Si^{4+} is ineffective or even counter-productive in the conversion of chromium ions to the tetravalent state [72].

Both Mg^{2+} and Ca^{2+} offer charge compensation for Cr^{4+} ions, although MgO appears to be more promising, due to ionic radius of Mg^{2+} that is similar to Al^{3+} [116]. As in the case of mixing SiO_2 with the divalent additives, also the mixture of CaO and MgO has been tested and provided promising results [128].

Based on the paper by Zhou et al. [80], Balashov et al. [130] used the molar ratio of Ca:Mg = 4:1 (but in contrast to Zhou et al., who used 0.2 mol.% total addition of CaO and MgO, 0.1 mol.% was used) for a successful preparation of highly transparent samples of Cr:YAG, Nd:YAG and Yb:YAG. In the case of Cr:YAG, the addition was on one hand optimal to achieve high transparency, but on the other hand, the conversion of Cr^{3+} to Cr^{4+} was not sufficient, even after annealing at 1400 °C in oxygen enriched atmosphere for 10 h. A more promising approach for Cr^{4+}:YAG seems to be the one applied by Zhou et al., who reached not only high transparency but also sufficient conversion of Cr^{3+} to Cr^{4+} by using Ca:Mg = 1:1 and with annealing temperature 1300 °C for 10 h in air and 1:0.93 ratio and annealing temperature 1300 °C for 30 h in oxygen [131].

Another point of view may be provided by the assessment of the effect of the molar ratio of Ca and Mg to Cr, $R = (n_{Ca} + n_{Mg})/n_{Cr}$. Surprisingly, Zhou et al. [80] reported that the conversion efficiency of chromium ions was higher for $R = 2$ than for $R = 1$, and that the conversion efficiency is not proportional to amount of charge compensators. Besides that, it was found out that R should be ≤ 2 [80].

The use of different amounts of CaO was studied by Chaika et al. [81], who found out that (besides the effects of CaO on the overall transparency and its function as sintering aid – see Section 2 of present paper) the efficiency of chromium conversion to Cr^{4+} does not depend monotonically on the Ca amount and that use of 0.5 at.% Ca leads to the best

Table 1
Illustration of the different sintering aids used in various transparent ceramics.

Material	Sintering aid	Typical amount added	Densification process	Ref.
Al_2O_3	MgO	0.05 wt%	sintering in H_2	[57, 122]
	$MgO + Y_2O_3$	0.05 wt% + 0.05 wt%		[57, 122]
	$MgO + Y_2O_3 + La_2O_3$	0.05 wt.% + 0.05 wt% + 0.05 wt%		[57, 122]
	Mg, Y, La and all their combinations, introduced as nitrates $Mg(NO_3)_2 \cdot 6H_2O$	0.045 wt% total	SPS	[10]
YAG	TEOS	0.05–0.3 wt% (corresponding to 0.17–1 wt% of TEOS)	vac, vac + HIP	[32,33, 35,39, 40,49, 50,123]
	MgO	0.03–0.05 wt%	vac	[60,63, 82]
	CaO	0.028–0.14 wt %	vac	[79,82]
	CaO + MgO	0.04 mol.% CaO + 0.16 mol.% MgO	vac	[69]
	SiO_2 + MgO	0.11–0.15 wt% SiO_2 + 0.08–0.1 wt% MgO	vac, vac. + HIP	[34,70, 71,73, 124]
	$SiO_2 + B_2O_3$	0.1 wt% TEOS + 0.4 wt% B_2O_3	vac	[89, 125, 126]
		0.34–1.31 wt% (different ratios of B^{3+}:Si^{4+})		[89]
	LiF	0.25 wt%	SPS	[99, 111]
	La_2O_3 + TEOS	0.8 wt% + N/A	vac	[85]
LuAG	SiO_2	0.14–0.28 wt%	vac	[53]
	MgO	0.02 wt%	vac	[66,67]
	SiO_2 + MgO	0.2 wt% TEOS + 0.08 wt% MgO	vac	[87]
	$Sc_2O_3 + La_2O_3$	0.4 wt% Sc_2O_3 + 0.6 wt% La_2O_3	vac	[87]
TAG	SiO_2 + MgO	0.4 wt% TEOS + 0.1 wt% MgO	vac, vac + HIP	[75,77]
	SiO_2	0.5 wt% TEOS	vac + HIP	[127]
GGAG	SiO2	0.5 wt% TEOS	air + HIP	[55]
Spinel	LiF	0.25–1.5 wt%, mostly 1 wt%	HP	[19,97, 101, 102, 106, 107, 112, 113]
	LiF	1 wt%	SPS	[107]
	NaF	1 wt%	SPS	[107]
	MgF_2	2.5 wt%	HP	[100]
	MgF_2	1.5 wt% MgF_2 + 0.5 wt% LiF	HP	[100]
	B_2O_3	0.08–0.15 wt%	vac + HIP	[90]
Y_2O_3	ZrO_2	3 mol. %	vac	[84,91]
	ZrO_2 + MgO	1.6 wt% ZrO_2 + 0.1 wt% MgO	vac	[92]
	LiF	1 wt%	HP	[114]
	LiF	0.3 wt%	SPS	[116]
Lu_2O_3	LiF	0.2 wt%	SPS	[118]

In the densification process description, *vac.* stands for vacuum sintering, *HP* for Hot Pressing, *HIP* for Hot Isostatic Pressing, *SPS* for Spark Plasma Sintering and *H_2* for sintering in H_2 atmosphere.

outcome both in the sense of highest transparency and Cr ions conversion. Chen et al. [72] also reported that CaO is effective charge compensator in Cr:YAG and sintering aid preventing pore formation and increasing homogeneity of microstructure. Ideal composition for high transparency and conversion efficiency of 0.25 at.% Cr:YAG in this case was found to be 0.05 wt% of CaO.

Another factor studied by Zhou et al. [129] that may have impact on the resulting optical properties is the particle size of the sintering aids. It was found that finer particles of sintering aids are beneficial to a higher conversion efficiency of chromium ions.

Nevertheless, besides the charge compensator kind, concentration and particle size, it should be kept in mind, that annealing conditions also have crucial impact on Cr^{3+} to Cr^{4+} conversion. Prolonged soaking times (up to 30 h), temperatures around 1300 °C and oxygen atmosphere are reported to be beneficial [129].

In scintillators, the use of MgO as a sintering aid in vacuum-sintered Ce:LuAG not only improved the optical quality, but provided an enhancement of the scintillation performance due to the presence of Ce^{4+} ions, stabilized by Mg^{2+} [132].

4. Secondary phases and other issues

While they are indispensable for the achievement of full transparency of various ceramics, it was noted that the introduction of sintering additives has also its downsides. Especially for certain applications like laser sources or scintillators, the presence of any impurity, including sintering aids, may be deleterious to the performance of the material [65, 74,133].

After sintering in a reducing atmosphere (e.g. vacuum sintering, HIP), the ceramics may suffer from parasitic absorption, visible as coloration (darkening or a hue from yellow to red or brown), often ascribed to the presence of oxygen vacancies [32,134] or metal ions in reduced states [135] In some cases the cause is clear, e.g. the green colour of vacuum sintered Yb:YAG samples due to the reduction of Yb^{3+} to Yb^{2+}, or the colour difference caused by the presence of Cr ions in different oxidation states, as described above, both requiring a further oxidating annealing treatment). On the other hand, sometimes the explanation is not so straightforward, as in the case of YAG samples, which gained a reddish coloration after sintering under a reducing atmosphere. This is illustrated in Fig. 4, where the presented YAG samples contained Si (0.5 wt% TEOS) and a small amount of Zr (introduced by the milling process). After vacuum sintering the samples had a red colour (left), which disappeared after air annealing (right). This effect has been observed also by Goldstein et al. [135], who ascribed it to the presence of the reduced Y^{2+} ions. In a recent article, Goldstein et al. [136] revised the previous work, explaining the mechanism further as promoted by the presence of tetravalent ions, which may be introduced as sintering aids, that cause lattice distortion in YAG. Interestingly, while Goldstein observed the red coloration in the case of Si-containing YAG samples sintered by HIP [136], the authors of this paper saw the effect in vacuum-sintered samples containing both Si and Zr (see Fig. 4), but not in samples containing only Si prepared under the same conditions. A relation between the red coloration in YAG and Zr has been observed also by Palmero et al. [134] for SPS-sintered YAG. Therefore, while the straining of the YAG lattice

Fig. 4. Photograph of YAG ceramics containing Si (0.5 wt% TEOS) and a small amount of Zr (introduced by milling process) sintered in vacuum at 1735 °C; after vacuum sintering, the sample has a red coloration (left), which disappears after annealing in air (right). (For interpretation of the references to color in this figure legend, the reader is referred to the Web version of this article.)

certainly occurs, and the coloration (parasitic absorption) is related to the presence of sintering aids, the explanation for the coloration is not necessarily the simple presence of Y^{2+} ions.

A common issue arising with the addition of sintering aids is the segregation of secondary phases or the compositional variation between the grains and grain boundaries [47,101,137]. Taking as an example YAG ceramics with SiO_2 sintering aid, Si-rich secondary phases have been observed [38,47,137,138] and Gaumé et al. reported the presence of Si-induced colour centres in YAG ceramics [133]. The presence of secondary phases may be limited by a good homogenisation and dispersion of the sintering aid. A typical example is the use of TEOS as a precursor for the formation of SiO_2, or the use of colloidal silica. However, even the "optimal" amount necessary for the achievement of full transparency may lead to grain boundary segregation, when the material contains certain dopants, e.g. Nd:YAG [44], Ce:YAG [45], or when the thermal treatment is not optimised, e.g. when the cooling rate in vacuum-sintered YAG ceramics with TEOS is too low [31], or when pressure is applied too early in the case of a hot-pressed spinel with LiF [106]. In the quest for a perfect material, transparency is thus not the only goal. The sintering aids need to be chosen carefully, taking into account not only the host material, but also the dopant. And in the search for defect-free ceramics, researchers are passing from percentage to ppm in the use of sintering aids, as long as the optical quality and uniformity of the material is not compromised.

Eventually, at least in the case of SiO_2 in YAG and LiF in spinel, there has been a series of works dealing with the sintering mechanisms and especially in the former case, also by the solubility of the sintering aid. After the older studies of Sun et al. [139] and Kuru et al. [140] on the solubility of Si YAG at 1550 °C and in a powder treated at 900 °C, respectively, more relevant data has been provided by Zamir [29], Ikesue et al. [31] and Boulesteix et al. [41], while Goldstein et al. studied the solubility of LiF in $MgAl_2O_4$ spinel [100]. For SiO_2 in YAG, the reduction of the amount of sintering aid was tackled in Section 2 of this article. Nevertheless, the amount initially added to the material is not necessarily the one in the sintered material. From the research on YAG and Nd:YAG ceramics with SiO_2 or TEOS added as a sintering aid it results that there is a significant decrease in the amount of silicon during the vacuum sintering process [31,41,43]. Moreover, the remaining amount of Si in the material depends on the cooling rate after sintering, as observed by Zamir [29], who investigated the solubility of Si in YAG at high temperatures. It was shown that the solubility limit is higher at high temperature, and after a fast quenching (200 °C/s), the amount of Si in the ceramic was higher compared to that in furnace-cooled (150 °C/h) samples. No second phases were observed in the quenched samples and only a small amount at triple junctions in the furnace-cooled samples. The effect of cooling rate was observed also by Ikesue et al. [3] in Nd:YAG, where an increasing amount Si-rich grain boundary phase was observed with the decrease of cooling rate (from 150 °C/h to 10 °C/h). Zamir also suggests that the heating rate affects the total amount of Si in the ceramic. This can be explained by the formation of volatile SiO in the reducing atmosphere of a vacuum furnace. Boulesteix et al. [41] observed a drop in Si content between 1400 and 1700 °C during vacuum sintering in samples with a higher initial SiO_2 content (0.3 wt% SiO_2, corresponding to about 1400 ppm of Si); interestingly, the authors showed that silica can be introduced from an external source (here by placing a Si-doped samples close to a Si-free one) during the sintering process. A similar process was conducted by Meir et al. with spinel sample exposed to LiF vapours, thus achieving transparency [105].

The use of MgO in YAG might appear promising given the lower additions when compared to SiO_2. However, at the same time the lower solubility limit of Mg^{2+} in YAG can lead to the formation of secondary phases with lower additions, as was described in Section 2.

Another example is transparent $MgAl_2O_4$ ceramics prepared with LiF as sintering aid. Since one of its main applications is transparent armour, high hardness and fracture toughness are beneficial. It is well known that those properties improve with decreasing grain size; however, the addition of LiF results in excessive grain growth. Even if nanosized powder is used as starting material, the final grain size can be in tens to hundreds of micrometres [109,141].

The use of SPS for the production proposes the possible elimination of sintering aids, or at least a significant reduction of the added quantities, as illustrated in Table 1. However, so far the optical quality is generally lower compared to more traditional approaches like vacuum sintering or HIP. Perhaps, one of the reasons can be that SPS provides the opportunity of very fast heating (>100 °C/min are possible), thus allowing to pass low temperature coarsening processes. Therefore, it is tempting to take advantage of this even in preparation of transparent ceramics; however, it seems that the complete removal of porosity is very much dictated by the total sintering time.

The group of Wu has recently presented the fabrication of transparent Yb:YAG without sintering aids by vacuum sintering, starting from co-precipitated powder [52]. This is yet another proof that the selection of the right starting powder may help to reduce, if not even eliminate the need for sintering aids for the densification process.

5. Conclusions

We have presented an overview of the different sintering aids and of the variety of transparent ceramics prepared with their addition. It was illustrated, how certain sintering aids are functional for specific sintering techniques (e.g. LiF for pressure-assisted sintering) or have a similar effect on different ceramic materials (e.g. MgO inhibiting grain growth). The combination of sintering aids proved promising, especially when one promotes densification and the other limits grain growth, providing thus a uniform microstructure and allowing the densification of larger pieces.

In some cases we suggest that the use of the term "sintering aid" should be used with consideration, like in the case of La_2O_3, which in a small amount helps obtaining a fine-grained uniform microstructure of Nd:YAG. On the other hand, when added to sesquioxides in a relatively high percentage (10%), La_2O_3 forms a mixed sesquioxide ceramic, and in such cases we would not consider this as a use of a sintering aid, although such suggestion are made in the literature.

In the last years, there has been a number of studies analysing more in detail the behaviour of sintering aids during the sintering process (LiF in spinel, SiO_2 in YAG) in order to understand the sintering mechanisms and the behaviour of the sintering aids during the sintering process, e.g. the Si solubility limit change under different cooling conditions or the discrepancy between the amount of Si introduced to the powder mixture and that remaining in the sintered material. It would be most helpful if similar studies were undertaken also for other systems, to shed more light into the empirical black boxes. From a practical viewpoint, while we know how much of a sintering aid is added into the mixture, there is an uncertainty about its presence in the sintered ceramic.

Declaration of competing interest

The authors declare that they have no known competing financial interests or personal relationships that could have appeared to influence the work reported in this paper.

Acknowledgements

J. H. gratefully acknowledges the following support: the scientific and technological research activity was co-financed by the Ministry of Defence within the framework of the National Military Research Plan (PNRM) managed by the Segretariato Generale della Difesa and the Direzione Nazionale degli Armamenti, Contract No. 8723 of December 19, 2014 (CeMiLAP) and Contract No. 8731 of December 04, 2019

(CeMiLAP^2), and by the Bilateral CNR/CAS project 2019–2021 "Thulium doped sesquoxide transparent ceramics for high energy class laser in nano second regime at cryogenic temperature".

S. H. and V. N. acknowledge support for this work, which is part of the project "Partially and fully sintered ceramics - processing, microstructure, properties, modeling and sintering theory" (GA18-17899S), supported by the Czech Science Foundation (GAČR).

The authors would like to thank Paolo Bassi for the work on the graphical abstract and Paolo Bassi would like to thank the authors for the fun of preparing it.

References

[1] A. Krell, T. Hutzler, J. Klimke, Transmission physics and consequences for materials selection, manufacturing, and applications, J. Eur. Ceram. Soc. 29 (2009) 207–221, https://doi.org/10.1016/j.jeurceramsoc.2008.03.025.

[2] W. Zhang, T. Lu, N. Wei, Y. Wang, B. Ma, F. Li, Z. Lu, J. Qi, Assessment of light scattering by pores in Nd:YAG transparent ceramics, J. Alloys Compd. 520 (2012) 36–41, https://doi.org/10.1016/j.jallcom.2011.12.012.

[3] A. Ikesue, K. Yoshida, T. Yamamoto, I. Yamaga, Optical scattering centers in polycrystalline Nd:YAG laser, J. Am. Ceram. Soc. 80 (1997) 1517–1522, https://doi.org/10.1111/j.1151-2916.1997.tb03011.x.

[4] K. Morita, B.N. Kim, K. Hiraga, H. Yoshida, Fabrication of high-strength transparent $MgAl_2O_4$ spinel polycrystals by optimizing spark-plasma-sintering conditions, J. Mater. Res. 24 (2009) 2836–2872, https://doi.org/10.1557/jmr.2009.0335.

[5] R. Boulesteix, A. Maître, J.-F. Baumard, Y. Rabinovitch, F. Reynaud, Light scattering by pores in transparent Nd:YAG ceramics for lasers: correlations between microstructure and optical properties, Opt Express 18 (2010) 14992–15002, https://doi.org/10.1364/oe.18.014992.

[6] Y. Wang, T. Lu, L. Gong, J. Qi, J. Wen, J. Yu, L. Pan, Y. Yu, N. Wei, Light extinction by pores in AlON ceramics: the transmission properties, J. Phys. D Appl. Phys. 43 (2010) 275403, https://doi.org/10.1088/0022-3727/43/27/275403.

[7] M. Stuer, P. Bowen, M. Cantoni, C. Pecharroman, Z. Zhao, Nanopore characterization and optical modeling of transparent polycrystalline alumina, Adv. Funct. Mater. 22 (2012) 2303–2309, https://doi.org/10.1002/adfm.201200123.

[8] S. Hříbalová, W. Pabst, Modeling light scattering by spherical pores for calculating the transmittance of transparent ceramics - all you need to know, J. Eur. Ceram. Soc. 41 (2020) 2169–2192, https://doi.org/10.1016/j.jeurceramsoc.2020.11.046.

[9] R.L. Coble, Sintering crystalline solids. I. intermediate and final state diffusion models, J. Appl. Phys. 32 (1961) 787–792, https://doi.org/10.1063/1.1736107.

[10] M. Stuer, Z. Zhao, U. Aschauer, P. Bowen, Transparent polycrystalline alumina using spark plasma sintering: effect of Mg, Y and La doping, J. Eur. Ceram. Soc. 30 (2010) 1335–1343, https://doi.org/10.1016/j.jeurceramsoc.2009.12.001.

[11] A. Krell, J. Klimke, T. Hutzler, Advanced spinel and sub-μm Al_2O_3 for transparent armour applications, J. Eur. Ceram. Soc. 29 (2009) 275–281, https://doi.org/10.1016/j.jeurceramsoc.2008.03.024.

[12] R. Apetz, M.P.B. Van Bruggen, Transparent alumina: a light-scattering model, J. Am. Ceram. Soc. 86 (2003) 480–486, https://doi.org/10.1111/j.1151-2916.2003.tb03325.x.

[13] C. Pecharromán, G. Mata-Osoro, L.A. Díaz, R. Torrecillas, J.S. Moya, On the transparency of nanostructured alumina: Rayleigh-Gans model for anisotropic spheres, Opt Express 17 (2009) 6899–6912, https://doi.org/10.1364/oe.17.006899.

[14] W. Pabst, S. Hříbalová, Light scattering models for describing the transmittance of transparent and translucent alumina and zirconia ceramics, J. Eur. Ceram. Soc. 41 (2021) 2058–2075, https://doi.org/10.1016/j.jeurceramsoc.2020.10.025.

[15] R.A. Lefever, J. Matsko, Transparent yttrium oxide ceramics, Mater. Res. Bull. 2 (1967) 865–869, https://doi.org/10.1016/0025-5408(67)90096-7.

[16] G. de With, H.J.A. van Dijk, Translucent $Y_3Al_5O_{12}$ ceramics, Mater. Res. Bull. 19 (1984) 1669–1674, https://doi.org/10.1016/0025-5408(84)90245-9.

[17] M. Sekita, H. Haneda, T. Yanagitani, S. Shirasaki, Induced emission cross section of Nd:$Y_3Al_5O_{12}$ ceramics, J. Appl. Phys. 67 (1990) 453–458, https://doi.org/10.1063/1.345224.

[18] A. Ikesue, T. Kinoshita, K. Kamata, K. Yoshida, Fabrication and optical properties of high-performance polycrystalline Nd:YAG ceramics for solid-state lasers, J. Am. Ceram. Soc. 78 (1995) 1033–1040, https://doi.org/10.1111/j.1151-2916.1995.tb08433.x.

[19] A. Goldstein, A. Krell, Transparent ceramics at 50: progress made and further prospects, J. Am. Ceram. Soc. 99 (2016) 3173–3197, https://doi.org/10.1111/jace.14553.

[20] S.F. Wang, J. Zhang, D.W. Luo, F. Gu, D.Y. Tang, Z.L. Dong, G.E.B. Tan, W.X. Que, T.S. Zhang, S. Li, L.B. Kong, Transparent ceramics: processing, materials and applications, Prog. Solid State Chem. 41 (2013) 20–54, https://doi.org/10.1016/j.progsolidstchem.2012.12.002.

[21] Z. Xiao, S. Yu, Y. Li, S. Ruan, L.B. Kong, Q. Huang, Z. Huang, K. Zhou, H. Su, Z. Yao, W. Que, Y. Liu, T. Zhang, J. Wang, P. Liu, D. Shen, M. Allix, J. Zhang, D. Tang, Materials development and potential applications of transparent ceramics: a review, Mater. Sci. Eng. R Rep. 139 (2020) 100518, https://doi.org/10.1016/j.mser.2019.100518.

[22] J. Hostaša, Ceramics for Laser Technologies, in: M. Pomeroy (Ed.), Encyclopedia of Materials: Technical Ceramics and Glasses 3, Elsevier, Oxford, 2021, pp. 110–124, https://doi.org/10.1016/B978-0-12-803581-8.11779-5.

[23] L.B. Kong, Y. Huang, W. Que, T. Zhang, S. Li, J. Zhang, Z. Dong, D. Tang, in: Transparent Ceramics, Springer, Switzerland, 2015, pp. 1–734, https://doi.org/10.1007/978-3-319-18956-7.

[24] A. Talimian, V. Pouchly, H.F. El-Maghraby, K. Maca, D. Galusek, Transparent magnesium aluminate spinel: effect of critical temperature in two-stage spark plasma sintering, J. Eur. Ceram. Soc. 40 (2020) 2417–2425, https://doi.org/10.1016/j.jeurceramsoc.2020.02.012.

[25] S. Grasso, H. Yoshida, H. Porwal, Y. Sakka, M. Reece, Highly transparent α-alumina obtained by low cost high pressure SPS, Ceram. Int. 39 (2013) 3243–3248, https://doi.org/10.1016/j.ceramint.2012.10.012.

[26] B.N. Kim, K. Hiraga, K. Morita, H. Yoshida, Spark plasma sintering of transparent alumina, Scripta Mater. 57 (2007) 607–610, https://doi.org/10.1016/j.scriptamat.2007.06.009.

[27] J. Sarthou, P. Aballéa, G. Patriarche, H. Serier-Brault, A. Suganuma, P. Gredin, M. Mortier, R. Riman, Wet-route synthesis and characterization of Yb:CaF_2 optical ceramics, J. Am. Ceram. Soc. 99 (2016) 1992–2000, https://doi.org/10.1111/jace.14216.

[28] M. Ivanov, E. Kalinina, Y. Kopylov, V. Kravchenko, I. Krutikova, U. Kynast, J. Li, M. Leznina, A. Medvedev, Highly transparent Yb-doped $(La_xY_{1-x})_2O_3$ ceramics prepared through colloidal methods of nanoparticles compaction, J. Eur. Ceram. Soc. 36 (2016) 4251–4259, https://doi.org/10.1016/j.jeurceramsoc.2016.06.013.

[29] S. Zamir, Solubility limit of Si in YAG at 1700 °C in vacuum, J. Eur. Ceram. Soc. 37 (2017) 243–248, https://doi.org/10.1016/j.jeurceramsoc.2016.08.010.

[30] S. Jiang, T. Lu, J. Chen, Ab initio study the effects of Si and Mg dopants on point defects and y diffusion in YAG, Comput. Mater. Sci. 69 (2013) 261–266, https://doi.org/10.1016/j.commatsci.2012.11.045.

[31] A. Ikesue, Y.L. Aung, in: Ceramic Lasers, Cambridge University Press, Cambridge, UK, 2010, https://doi.org/10.1017/CBO9780511978043.

[32] R. Boulesteix, A. Maître, L. Chrétien, Y. Rabinovitch, C. Sallé, Microstructural evolution during vacuum sintering of yttrium aluminum garnet transparent ceramics: toward the origin of residual porosity affecting the transparency, J. Am. Ceram. Soc. 96 (2013) 1724–1731, https://doi.org/10.1111/jace.12315.

[33] S. Kochawattana, A. Stevenson, S.H. Lee, M. Ramirez, V. Gopalan, J. Dumm, V.K. Castillo, G.J. Quarles, G.L. Messing, Sintering and grain growth in SiO_2 doped Nd:YAG, J. Eur. Ceram. Soc. 28 (2008) 1527–1534, https://doi.org/10.1016/j.jeurceramsoc.2007.12.006.

[34] X. Chen, Y. Wu, N. Wei, J. Qi, Z. Lu, Q. Zhang, T. Hua, Q. Zeng, T. Lu, The roles of cation additives on the color center and optical properties of Yb:YAG transparent ceramic, J. Eur. Ceram. Soc. 38 (2018) 1957–1965, https://doi.org/10.1016/j.jeurceramsoc.2017.11.055.

[35] A.J. Stevenson, X. Li, M.A. Martinez, J.M. Anderson, D.L. Suchy, E.R. Kupp, E.C. Dickey, K.T. Mueller, G.L. Messing, Effect of SiO_2 on densification and microstructure development in Nd:YAG transparent ceramics, J. Am. Ceram. Soc. 94 (2011) 1380–1387, https://doi.org/10.1111/j.1551-2916.2010.04260.x.

[36] M. Sekita, H. Haneda, S. Shirasaki, T. Yanagitani, Optical spectra of undoped and rare-earth-(=Pr, Nd, Eu, and Er) doped transparent ceramic $Y_3Al_5O_{12}$, J. Appl. Phys. 69 (1991) 3709–3718, https://doi.org/10.1063/1.348959.

[37] H. Yagi, T. Yanagitani, K.-I. Ueda, Nd^{3+}:$Y_3Al_5O_{12}$ laser ceramics: flashlamp pumped laser operation with a UV cut filter, J. Alloys Compd. 421 (2006) 195–199, https://doi.org/10.1016/j.jallcom.2005.09.083.

[38] R. Boulesteix, A. Maître, J.F. Baumard, Y. Rabinovitch, C. Sallé, S. Weber, M. Kilo, The effect of silica doping on neodymium diffusion in yttrium aluminum garnet ceramics: implications for sintering mechanisms, J. Eur. Ceram. Soc. 29 (2009) 2517–2526, https://doi.org/10.1016/j.jeurceramsoc.2009.03.003.

[39] R. Boulesteix, A. Maître, J.F. Baumard, C. Sallé, Y. Rabinovitch, Mechanism of the liquid-phase sintering for Nd:YAG ceramics, Opt. Mater. 31 (2009) 711–715, https://doi.org/10.1016/j.optmat.2008.04.005.

[40] S.H. Lee, E.R. Kupp, A.J. Stevenson, J.M. Anderson, G.L. Messing, X. Li, E.C. Dickey, J.Q. Dumm, V.K. Simonaitis-Castillo, G.J. Quarles, Hot isostatic pressing of transparent Nd:YAG ceramics, J. Am. Ceram. Soc. 92 (2009) 1456–1463, https://doi.org/10.1111/j.1551-2916.2009.03029.x.

[41] R. Boulesteix, L. Bonnet, A. Maître, L. Chrétien, C. Sallé, Silica reactivity during reaction-sintering of Nd:YAG transparent ceramics, J. Am. Ceram. Soc. 100 (2017) 945–953, https://doi.org/10.1111/jace.14680.

[42] S.J. Pandey, M. Martinez, J. Hostaša, L. Esposito, M. Baudelet, R.M. Gaume, Quantification of SiO_2 sintering additive in YAG transparent ceramics by laser-induced breakdown microscopy (LIBS), Opt. Mater. Express 7 (2017) 1666–1671, https://doi.org/10.1364/OME.7.001666.

[43] J. Hostaša, A. Piancastelli, V. Biasini, S.J. Pandey, M. Martinez, M. Baudelet, R. Gaume, Advances in the monitoring of the SiO_2 evaporation loss in transparent YAG ceramics by LIBS, Ceram. Int. 45 (2019) 12274–12278, https://doi.org/10.1016/j.ceramint.2019.03.140.

[44] M.O. Ramirez, J. Wisdom, H. Li, Y.L. Aung, J. Stitt, G.L. Messing, V. Dierolf, Z. Liu, A. Ikesue, R.L. Byer, V. Gopalan, Three-dimensional grain boundary spectroscopy in transparent high power ceramic laser materials, Opt Express 16 (2008) 5965–5973, https://doi.org/10.1364/oe.16.005965.

[45] W. Zhao, S. Anghel, C. Mancini, D. Amans, G. Boulon, T. Epicier, Y. Shi, X.Q. Feng, Y.B. Pan, V. Chani, A. Yoshikawa, Ce^{3+} dopant segregation in $Y_3Al_5O_{12}$ optical ceramics, Opt. Mater. 33 (2011) 684–687, https://doi.org/10.1016/j.optmat.2010.10.007.

[46] L. Esposito, J. Hostaša, A. Piancastelli, G. Toci, D. Alderighi, M. Vannini, T. Epicier, A. Malchère, G. Alombert-Goget, G. Boulon, Multilayered YAG-Yb:YAG

ceramics: manufacture and laser performance, J. Mater. Chem. C. 2 (2014) 10138–10148, https://doi.org/10.1039/c4tc01544d.
[47] T. Epicier, G. Boulon, W. Zhao, M. Guzik, B. Jiang, A. Ikesue, L. Esposito, Spatial distribution of the Yb^{3+} rare earth ions in $Y_3Al_5O_{12}$ and Y_2O_3 optical ceramics as analyzed by TEM, J. Mater. Chem. 35 (2012) 18221–18229, https://doi.org/10.1039/c2jm32995f.
[48] S. Zamir, Si segregation and its role in reaching transparent YAG, J. Am. Ceram. Soc. 100 (2017) 1689–1696, https://doi.org/10.1111/jace.14621.
[49] J. Hostaša, L. Esposito, A. Piancastelli, Influence of Yb and Si content on the sintering and phase changes of Yb:YAG laser ceramics, J. Eur. Ceram. Soc. 32 (2012) 2949–2956, https://doi.org/10.1016/j.jeurceramsoc.2012.02.045.
[50] P. Ma, N. Jiang, C. Li, T. Xie, H. Kou, Y. Shi, H. Chen, Y. Pan, J. Li, S. Li, X. Zhu, M. Ivanov, D. Hreniak, Post-treatment of nanopowders-derived Nd:YAG transparent ceramics by hot isostatic pressing, Ceram. Int. 43 (2017) 10013–10019, https://doi.org/10.1016/j.ceramint.2017.05.015.
[51] A. Ikesue, Y.L. Aung, Synthesis of Yb:YAG ceramics without sintering additives and their performance, J. Am. Ceram. Soc. 100 (2017) 26–30, https://doi.org/10.1111/jace.14588.
[52] X. Chen, T. Lu, N. Wei, T. Hua, Q. Zeng, Y. Wu, Fabrication and microstructure development of Yb:YAG transparent ceramics from co-precipitated powders without additives, J. Am. Ceram. Soc. 102 (2019) 7154–7167, https://doi.org/10.1111/jace.16635.
[53] L. Basyrova, R. Maksimov, V. Shitov, M. Baranov, V. Mikhaylovsky, A. Khubetsov, O. Dymshits, X. Mateos, P. Loiko, Effect of SiO_2 addition on structural and optical properties of Yb:$Lu_3Al_5O_{12}$ transparent ceramics based on laser ablated nanopowders, J. Alloys Compd. 806 (2019) 717–725, https://doi.org/10.1016/j.jallcom.2019.07.285.
[54] L. Bonnet, R. Boulesteix, A. Maître, C. Sallé, V. Couderc, A. Brenier, Manufacturing issues and optical properties of rare-earth (Y, Lu, Sc, Nd) aluminate garnets composite transparent ceramics, Opt. Mater. 50 (2015) 2–10, https://doi.org/10.1016/j.optmat.2015.04.050.
[55] J. Hostaša, F. Cova, A. Piancastelli, M. Fasoli, C. Zanelli, A. Vedda, V. Biasini, Fabrication and luminescence of Ce-doped GGAG transparent ceramics, effect of sintering parameters and additives, Ceram. Int. 45 (2019) 23283–23288, https://doi.org/10.1016/j.ceramint.2019.08.025.
[56] X. Huang, L. Zuo, X. Li, Y. Feng, X. Liu, X. Chen, T. Xie, Z. Yang, L. Wu, J. Li, Fabrication and characterization of $Tb_3Al_5O_{12}$ magneto-optical ceramics by solid-state reactive sintering, Opt. Mater. 102 (2020) 109795, https://doi.org/10.1016/j.optmat.2020.109795.
[57] R.L. Coble, Sintering crystalline solids. II. experimental test of diffusion models in powder compacts, J. Appl. Phys. 32 (1961) 793–799, https://doi.org/10.1063/1.1736108.
[58] K.A. Berry, M.P. Harmer, Effect of MgO solute on microstructure development in Al_2O_3, J. Am. Ceram. Soc. 69 (1986) 143–149, https://doi.org/10.1111/j.1151-2916.1986.tb04719.x.
[59] D.S. Kim, J.H. Lee, R.J. Sung, S.W. Kim, H.S. Kim, J.S. Park, Improvement of translucency in Al_2O_3 ceramics by two-step sintering technique, J. Eur. Ceram. Soc. 27 (2007) 3629–3632, https://doi.org/10.1016/j.jeurceramsoc.2007.02.002.
[60] T.Y. Zhou, L. Zhang, S. Wei, L.X. Wang, H. Yang, Z.X. Fu, H. Chen, F.A. Selim, Q.T. Zhang, MgO assisted densification of highly transparent YAG ceramics and their microstructural evolution, J. Eur. Ceram. Soc. 38 (2018) 687–693, https://doi.org/10.1016/j.jeurceramsoc.2017.09.017.
[61] S. Zamir, The influence of cation additives on grain-boundary mobility in Yttrium Aluminum Garnet (YAG), J. Am. Ceram. Soc. 98 (2015) 324–330, https://doi.org/10.1111/jace.13290.
[62] A.G. Doroshenko, R.P. Yavetskiy, S.V. Parkhomenko, I.O. Vorona, O.S. Kryzhanovska, P.V. Mateychenko, A.V. Tolmachev, E.A. Vovk, V.A. Bovda, G. Croitoru, L. Gheorghe, Effect of the sintering temperature on the microstructure and optical properties of YAG:Cr,Mg ceramics, Opt. Mater. 98 (2019) 109505, https://doi.org/10.1016/j.optmat.2019.109505.
[63] I. Vorona, A. Balabanov, M. Dobrotvorska, R. Yavetskiy, O. Kryzhanovska, L. Kravchenko, S. Parkhomenko, P. Mateychenko, V. Baumer, I. Matolínová, Effect of MgO doping on the structure and optical properties of YAG transparent ceramics, J. Eur. Ceram. Soc. 40 (2020) 861–866, https://doi.org/10.1016/j.jeurceramsoc.2019.10.048.
[64] M.A. Chaika, O.M. Vovk, A.G. Doroshenko, V.K. Klochkov, P.V. Mateychenko, S.V. Parkhomenko, O.G. Fedorov, Influence of Ca and Mg doping on the microstructure and optical properties of YAG ceramics, Met. Funct. Mater. 24 (2017) 237–243, https://doi.org/10.15407/fm24.02.237.
[65] M. Buryi, L. Havlák, V. Jarý, J. Bárta, V. Laguta, A. Beitlerová, J. Li, X. Chen, Y. Yuan, Q. Liu, Y. Pan, M. Nikl, Specific absorption in $Y_3Al_5O_{12}$:Eu ceramics and the role of stable Eu^{2+} in energy transfer processes, J. Mater. Chem. C. 8 (2020) 8823–8839.
[66] S. Liu, J.A. Mares, V. Babin, C. Hu, H. Kou, C. D'Ambrosio, J. Li, Y. Pan, M. Nikl, Composition and properties tailoring in Mg^{2+} codoped non-stoichiometric LuAG: Ce,Mg scintillation ceramics, J. Eur. Ceram. Soc. 37 (2017) 1689–1694, https://doi.org/10.1016/j.jeurceramsoc.2016.10.023.
[67] P. Zhang, B. Chai, B. Jiang, Y. Jiang, S. Chen, Q. Gan, J. Fan, X. Mao, L. Zhang, High transparency Cr,Nd:LuAG ceramics prepared with MgO additive, J. Eur. Ceram. Soc. 37 (2017) 2459–2463, https://doi.org/10.1016/j.jeurceramsoc.2017.01.023.
[68] Z. Hu, M. Cao, H. Chen, Y. Shi, H. Kou, T. Xie, L. Wu, Y. Pan, X. Feng, A. Vedda, A. Beitlerova, M. Nikl, J. Li, The role of air annealing on the optical and scintillation properties of Mg co-doped Pr:LuAG transparent ceramics, Opt. Mater. 72 (2017) 201–207, https://doi.org/10.1016/j.optmat.2017.05.054.
[69] T. Zhou, L. Zhang, F.A. Selim, R. Sun, C. Wong, H. Chen, Q. Zhang, Annealing induced discoloration of transparent YAG ceramics using divalent additives in solid-state reaction sintering, J. Eur. Ceram. Soc. 37 (2017) 4123–4128, https://doi.org/10.1016/j.jeurceramsoc.2017.05.030.
[70] H. Yang, X. Qin, J. Zhang, J. Ma, D. Tang, S. Wang, Q. Zhang, The effect of MgO and SiO_2 codoping on the properties of Nd:YAG transparent ceramic, Opt. Mater. 34 (2012) 940–943, https://doi.org/10.1016/j.optmat.2011.05.029.
[71] F. Mohammadi, O. Mirzaee, M. Tajally, Influence of TEOS and MgO addition on slurry rheological, optical, and microstructure properties of YAG transparent ceramic, Opt. Mater. 85 (2018) 174–182, https://doi.org/10.1016/j.optmat.2018.08.047.
[72] X.T. Chen, Y.Q. Wu, Z.W. Lu, N. Wei, J.Q. Qi, Y.L. Shi, T.F. Hua, Q. Zeng, W. Guo, T.C. Lu, Assessment of conversion efficiency of Cr^{4+} ions by aliovalent cation additives in Cr:YAG ceramic for edge cladding, J. Am. Ceram. Soc. 101 (2018) 5098–5109, https://doi.org/10.1111/jace.15764.
[73] W. Liu, W. Zhang, J. Li, H. Kou, D. Zhang, Y. Pan, Synthesis of Nd:YAG powders leading to transparent ceramics: the effect of MgO dopant, J. Eur. Ceram. Soc. 31 (2011) 653–657, https://doi.org/10.1016/j.jeurceramsoc.2010.10.016.
[74] Y. Shen, Y. Shi, X. Feng, Y. Pan, J. Li, Y. Zeng, M. Nikl, A. Krasnikov, A. Vedda, F. Moretti, The harmful effects of sintering aids in Pr:LuAG optical ceramic scintillator, J. Am. Ceram. Soc. 95 (2012) 2130–2132, https://doi.org/10.1111/j.1551-2916.2012.05275.x.
[75] C. Chen, X. Yi, S. Zhang, Y. Feng, Y. Tang, H. Lin, S. Zhou, Vacuum sintering of $Tb_3Al_5O_{12}$ transparent ceramics with combined TEOS+MgO sintering aids, Ceram. Int. 41 (2015) 12823–12827, https://doi.org/10.1016/j.ceramint.2015.06.118.
[76] D. Hao, X. Shao, Y. Tang, X. Yi, J. Chen, S. Zhou, Effect of Si^{4+} doping on the microstructure and magneto-optical properties of TAG transparent ceramics, Opt. Mater. 77 (2018) 253–257, https://doi.org/10.1016/j.optmat.2018.01.049.
[77] S. Zhang, P. Liu, X. Xu, J. Zhang, Effect of the MgO on microstructure and optical properties of TAG ($Tb_3Al_5O_{12}$) transparent ceramics using hot isostatic pressing, Opt. Mater. 80 (2018) 7–11, https://doi.org/10.1016/j.optmat.2018.04.032.
[78] T.F. Hua, Q. Zeng, J.Q. Qi, G. Cheng, X.T. Chen, Z.Y. Huang, Q.H. Zhang, X. Huang, X.F. Guo, N. Wei, T.C. Lu, Effect of calcium oxide doping on the microstructure and optical properties of YAG transparent ceramics, Mater. Res. Express 6 (2019), 036203, https://doi.org/10.1088/2053-1591/aaf487.
[79] L. Zhang, T. Zhou, F.A. Selim, H. Chen, Single CaO accelerated densification and microstructure control of highly transparent YAG ceramic, J. Am. Ceram. Soc. 101 (2018) 703–712, https://doi.org/10.1111/jace.15233.
[80] T.Y. Zhou, L. Zhang, Z. Li, S. Wei, J.D. Wu, L.X. Wang, H. Yang, Z.X. Fu, H. Chen, D.Y. Tang, C.P. Wong, Q.T. Zhang, Toward vacuum sintering of YAG transparent ceramic using divalent dopant as sintering aids: investigation of microstructural evolution and optical property, Ceram. Int. 43 (2017) 3140–3146, https://doi.org/10.1016/j.ceramint.2016.11.131.
[81] M.A. Chaika, N.A. Dulina, A.G. Doroshenko, S.V. Parkhomenko, O.V. Gayduk, R. Tomala, W. Strek, D. Hreniak, G. Mancardi, O.M. Vovk, Influence of calcium concentration on formation of tetravalent chromium doped $Y_3Al_5O_{12}$ ceramics, Ceram. Int. 44 (2018) 13513–13519, https://doi.org/10.1016/j.ceramint.2018.04.182.
[82] M.A. Chaika, G. Mancardi, R. Tomala, W. Stek, O.M. Vovk, Effects of divalent dopants on the microstructure and conversion efficiency of Cr^{4+} ions in Cr,Me: YAG (Me – Ca, Mg, Ca/Mg) transparent ceramics, Process. Appl. Ceram. 14 (2020) 83–89, https://doi.org/10.2298/PAC2001083C.
[83] X. Hu, Q. Yang, C. Dou, J. Xu, H. Zhou, Fabrication and spectral properties of Nd^{3+}-doped yttrium lanthanum oxide transparent ceramics, Opt. Mater. 30 (2008) 1583–1586, https://doi.org/10.1016/j.optmat.2007.10.008.
[84] Q. Yi, S. Zhou, H. Teng, H. Lin, X. Hou, T. Jia, Structural and optical properties of Tm:Y_2O_3 transparent ceramic with La_2O_3, ZrO_2 as composite sintering aid, J. Eur. Ceram. Soc. 32 (2012) 381–388, https://doi.org/10.1016/j.jeurceramsoc.2011.09.015.
[85] W. Liu, J. Li, B. Jiang, D. Zhang, Y. Pan, Effect of La_2O_3 on microstructures and laser properties of Nd:YAG ceramics, J. Alloys Compd. 512 (2012) 1–4, https://doi.org/10.1016/j.jallcom.2011.09.038.
[86] W. Liu, Y. Zeng, J. Li, Y. Shen, Y. Bo, N. Zong, P. Wang, Y. Xu, J. Xu, D. Cui, Q. Peng, Z. Xu, D. Zhang, Y. Pan, Sintering and laser behavior of composite YAG/Nd:YAG/YAG transparent ceramics, J. Alloys Compd. 527 (2012) 66–70, https://doi.org/10.1016/j.jallcom.2012.02.161.
[87] Y. Shen, X. Feng, V. Babin, M. Nikl, A. Vedda, F. Moretti, E. Dell'Orto, Y. Pan, J. Li, Y. Zeng, Fabrication and scintillation properties of highly transparent Pr:LuAG ceramics using Sc,La-based isovalent sintering aids, Ceram. Int. 39 (2013) 5985–5990, https://doi.org/10.1016/j.ceramint.2012.12.065.
[88] B. Jiang, X. Lu, Y. Zeng, S. Liu, J. Li, W. Liu, Y. Shi, Y. Pan, Synthesis and properties of Yb:LuAG transparent ceramics, Phys. Status Solidi Curr. Top. Solid State Phys. 10 (2013) 958–961, https://doi.org/10.1002/pssc.201300016.
[89] A.J. Stevenson, E.R. Kupp, G.L. Messing, Low temperature, transient liquid phase sintering of B_2O_3-SiO_2-doped Nd:YAG transparent ceramics, J. Mater. Res. 26 (2011) 1151–1158, https://doi.org/10.1557/jmr.2011.45.
[90] K. Tsukuma, Transparent $MgAl_2O_4$ spinel ceramics produced by HIP post-sintering, J. Ceram. Soc. Jpn. 114 (2006) 802–806, https://doi.org/10.2109/jcersj.114.802.
[91] W.K. Jung, H.J. Ma, Y. Park, D.K. Kim, A robust approach for highly transparent Y_2O_3 ceramics by stabilizing oxygen defects, Scripta Mater. 137 (2017) 1–4, https://doi.org/10.1016/j.scriptamat.2017.04.036.
[92] K. Ning, J. Wang, D. Luo, J. Zhang, Z.L. Dong, L.B. Kong, D.Y. Tang, New double-sintering aid for fabrication of highly transparent ytterbium-doped yttria ceramics, J. Eur. Ceram. Soc. 36 (2016) 253–256, https://doi.org/10.1016/j.jeurceramsoc.2015.09.007.

[93] R.P. Yavetskiy, D.Y. Kosyanov, A.G. Doroshenko, S.V. Parkhomenko, P.V. Mateychenko, I.O. Vorona, A.V. Tolmachev, A.V. Lopin, V.N. Baumer, V.L. Voznyy, Microstructure evolution of SiO_2, ZrO_2-doped $Y_3Al_5O_{12}$:Nd^{3+} ceramics obtained by reactive sintering, Ceram. Int. 41 (2015) 11966–11974, https://doi.org/10.1016/j.ceramint.2015.06.009.

[94] K. Morita, B.N. Kim, H. Yoshida, K. Hiraga, Y. Sakka, Distribution of carbon contamination in oxide ceramics occurring during spark-plasma-sintering (SPS) processing: II - effect of SPS and loading temperatures, J. Eur. Ceram. Soc. 38 (2018) 2596–2604, https://doi.org/10.1016/j.jeurceramsoc.2017.12.004.

[95] K. Morita, B.N. Kim, H. Yoshida, K. Hiraga, Y. Sakka, Distribution of carbon contamination in $MgAl_2O_4$ spinel occurring during spark-plasma-sintering (SPS) processing: I – effect of heating rate and post-annealing, J. Eur. Ceram. Soc. 38 (2018) 2588–2595, https://doi.org/10.1016/j.jeurceramsoc.2017.09.038.

[96] K. Morita, B.N. Kim, H. Yoshida, K. Hiraga, Y. Sakka, Assessment of carbon contamination in $MgAl_2O_4$ spinel during spark-plasma-sintering (SPS) processing, J. Ceram. Soc. Japan. 123 (2015) 983–988, https://doi.org/10.2109/jcersj2.123.983.

[97] M. Rubat Du Merac, H.J. Kleebe, M.M. Müller, I.E. Reimanis, Fifty years of research and development coming to fruition; Unraveling the complex interactions during processing of transparent magnesium aluminate ($MgAl_2O_4$) spinel, J. Am. Ceram. Soc. 96 (2013) 3341–3365, https://doi.org/10.1111/jace.12637.

[98] I. Ganesh, K.A. Teja, N. Thiyagarajan, R. Johnson, B.M. Reddy, Formation and densification behavior of magnesium aluminate spinel: the influence of CaO and moisture in the precursors, J. Am. Ceram. Soc. 88 (2005) 2752–2761, https://doi.org/10.1111/j.1551-2916.2005.00529.x.

[99] N. Frage, S. Kalabukhov, N. Sverdlov, V. Kasiyan, A. Rothman, M.P. Dariel, Effect of the spark plasma sintering (SPS) parameters and LiF doping on the mechanical properties and the transparency of polycrystalline Nd-YAG, Ceram. Int. 38 (2012) 5513–5519, https://doi.org/10.1016/j.ceramint.2012.03.066.

[100] A. Goldstein, J. Raethel, M. Katz, M. Berlin, E. Galun, Transparent $MgAl_2O_4$/LiF ceramics by hot-pressing: host-additive interaction mechanisms issue revisited, J. Eur. Ceram. Soc. 36 (2016) 1731–1742, https://doi.org/10.1016/j.jeurceramsoc.2016.02.001.

[101] S.S. Balabanov, A.V. Belyaev, A.V. Novikova, D.A. Permin, E.Y. Rostokina, R.P. Yavetskiy, Densification peculiarities of transparent $MgAl_2O_4$ ceramics - effect of LiF sintering additive, Inorg. Mater. 54 (2018) 1045–1050, https://doi.org/10.1134/S0020168518100023.

[102] L. Esposito, A. Piancastelli, S. Martelli, Production and characterization of transparent $MgAl_2O_4$ prepared by hot pressing, J. Eur. Ceram. Soc. 33 (2013) 737–747, https://doi.org/10.1016/j.jeurceramsoc.2012.10.013.

[103] J. Sanghera, S. Bayya, G. Villalobos, W. Kim, J. Frantz, B. Shaw, B. Sadowski, R. Miklos, C. Baker, M. Hunt, I. Aggarwal, F. Kung, D. Reicher, S. Peplinski, A. Ogloza, P. Langston, C. Lamar, P. Varmette, M. Dubinskiy, L. Desandre, Transparent ceramics for high-energy laser systems, Opt. Mater. 33 (2011) 511–518, https://doi.org/10.1016/j.optmat.2010.10.038.

[104] J.L. Huang, S.Y. Sun, C.Y. Chen, Investigation of high alumina-spinel: effects of LiF and $CaCO_3$ addition (Part 2), Mater. Sci. Eng. 259 (1999) 1–7, https://doi.org/10.1016/S0921-5093(98)00881-8.

[105] S. Meir, S. Kalabukhov, N. Froumin, M.P. Dariel, N. Frage, Synthesis and densification of transparent magnesium aluminate spinel by SPS processing, J. Am. Ceram. Soc. 92 (2009) 358–364, https://doi.org/10.1111/j.1551-2916.2008.02893.x.

[106] L. Esposito, A. Piancastelli, P. Miceli, S. Martelli, A thermodynamic approach to obtaining transparent spinel ($MgAl_2O_4$) by hot pressing, J. Eur. Ceram. Soc. 35 (2015) 651–661, https://doi.org/10.1016/j.jeurceramsoc.2014.09.005.

[107] V. Nečina, W. Pabst, Comparison of the effect of different alkali halides on the preparation of transparent $MgAl_2O_4$ spinel ceramics via spark plasma sintering (SPS), J. Eur. Ceram. Soc. 40 (2020) 6043–6052, https://doi.org/10.1016/j.jeurceramsoc.2020.06.056.

[108] I.E. Reimanis, H.J. Kleebe, Reactions in the sintering of $MgAl_2O_4$ spinel doped with LiF, Int. J. Mater. Res. 98 (2007) 1273–1278, https://doi.org/10.3139/146.101591.

[109] I. Reimanis, H.J. Kleebe, A review on the sintering and microstructure development of transparent spinel ($MgAl_2O_4$), J. Am. Ceram. Soc. 92 (2009) 1472–1480, https://doi.org/10.1111/j.1551-2916.2009.03108.x.

[110] C.-J. Ting, H.-Y. Lu, Defect reactions and the controlling mechanism in the sintering of magnesium aluminate spinel, J. Am. Ceram. Soc. 88 (1999) 841–848, https://doi.org/10.1111/j.1151-2916.1999.tb01844.x.

[111] A. Katz, E. Barraud, S. Lemonnier, E. Sorrel, M. Eichhorn, S. d'Astorg, A. Leriche, Role of LiF additive on spark plasma sintered transparent YAG ceramics, Ceram. Int. 43 (2017) 15626–15634, https://doi.org/10.1016/j.ceramint.2017.08.119.

[112] K. Rozenburg, I.E. Reimanis, H.J. Kleebe, R.L. Cook, Sintering kinetics of a $MgAl_2O_4$ spinel doped with LiF, J. Am. Ceram. Soc. 91 (2008) 444–450, https://doi.org/10.1111/j.1551-2916.2007.02185.x.

[113] W. Luo, R. Xie, M. Ivanov, Y. Pan, H. Kou, J. Li, Effects of LiF on the microstructure and optical properties of hot-pressed $MgAl_2O_4$ ceramics, Ceram. Int. 43 (2017) 6891–6897, https://doi.org/10.1016/j.ceramint.2017.02.110.

[114] K. Majima, N. Niimi, M. Watanabe, S. Katsuyama, H. Nagai, Effect of LiF addition on the preparation of transparent Y_2O_3 by the vacuum hot pressing method, J. Alloys Compd. 193 (1993) 280–282, https://doi.org/10.1016/0925-8388(93)90371-S.

[115] X. Zhang, G. Fan, W. Lu, Y. Chen, X. Ruan, Effect of the spark plasma sintering parameters, LiF additive, and Nd dopant on the microwave dielectric and optical properties of transparent YAG ceramics, J. Eur. Ceram. Soc. 36 (2016) 2762–2772, https://doi.org/10.1016/j.jeurceramsoc.2016.04.029.

[116] Z. Hu, X. Xu, J. Wang, P. Liu, D. Li, X. Wang, J. Zhang, J. Xu, D. Tang, Fabrication and spectral properties of Dy:Y_2O_3 transparent ceramics, J. Eur. Ceram. Soc. 38 (2018) 1981–1985, https://doi.org/10.1016/j.jeurceramsoc.2017.12.020.

[117] Z. Hu, X. Xu, J. Wang, P. Liu, D. Li, X. Wang, L. An, J. Zhang, J. Xu, D. Tang, Spark plasma sintering of Sm^{3+} doped Y_2O_3 transparent ceramics for visible light lasers, Ceram. Int. 43 (2017) 12057–12060, https://doi.org/10.1016/j.ceramint.2017.06.059.

[118] G. Alombert-Goget, Y. Guyot, M. Guzik, G. Boulon, A. Ito, T. Goto, A. Yoshikawa, M. Kikuchi, Nd^{3+}-doped Lu_2O_3 transparent sesquioxide ceramics elaborated by the Spark Plasma Sintering (SPS) method. Part 1: structural, thermal conductivity and spectroscopic characterization, Opt. Mater. 41 (2015) 3–11, https://doi.org/10.1016/j.optmat.2014.10.014.

[119] N. Jiang, R.-j. Xie, Q. Liu, J. Li, Fabrication of sub-micrometer MgO transparent ceramics by spark plasma sintering, J. Eur. Ceram. Soc. 37 (2017) 4947–4953, https://doi.org/10.1016/j.jeurceramsoc.2017.06.021.

[120] I. Ganesh, S. Bhattacharjee, B.P. Saha, R. Johnson, Y.R. Mahajan, A new sintering aid for magnesium aluminate spinel, Ceram. Int. 27 (2001) 773–779, https://doi.org/10.1016/S0272-8842(01)00029-3.

[121] J. Fan, S. Chen, B. Jiang, L. Pan, Y. Zhang, X. Mao, X. Yuan, R. Li, X. Jiang, L. Zhang, Improvement of optical properties and suppression of second phase exsolution by doping fluorides in $Y_3Al_5O_{12}$ transparent ceramics, Opt. Mater. Express 4 (2014) 1800–1806, https://doi.org/10.1364/ome.4.001800.

[122] G. Liu, Z. Xie, W. Liu, L. Cheng, Y. Wu, Fabrication of translucent alumina ceramics from pre-sintered bodies infiltrated with sintering additive precursor solutions, J. Eur. Ceram. Soc. 32 (2012) 711–715, https://doi.org/10.1016/j.jeurceramsoc.2011.10.019.

[123] J. Hostaša, M. Schwentenwein, G. Toci, L. Esposito, D. Brouczek, A. Piancastelli, A. Pirri, B. Patrizi, M. Vannini, V. Biasini, Transparent laser ceramics by stereolithography, Scripta Mater. 187 (2020) 194–196, https://doi.org/10.1016/j.scriptamat.2020.06.006.

[124] Y. Li, S. Zhou, H. Lin, X. Hou, W. Li, H. Teng, T. Jia, Fabrication of Nd:YAG transparent ceramics with TEOS, MgO and compound additives as sintering aids, J. Alloys Compd. 502 (2010) 225–230, https://doi.org/10.1016/j.jallcom.2010.04.151.

[125] A.A. Kaminskii, V.V. Balashov, E.A. Cheshev, Y.L. Kopylov, A.L. Koromyslov, O.N. Krokhin, V.B. Kravchenko, K.V. Lopukhin, V.V. Shemet, High quality $Y_3Al_5O_{12}$ doped transparent ceramics for laser applications, role of sintering additives, Opt. Mater. 71 (2017) 103–108, https://doi.org/10.1016/j.optmat.2016.05.015.

[126] Y. Yang, C. Yang, X. Li, D. Zhou, Influence of B_2O_3/SiO_2 ratio on the fabrication of Nd:YAG ceramics, Integrated Ferroelectrics Int. J. 159 (2015) 66–72, https://doi.org/10.1080/10584587.2015.1031056.

[127] J. Dai, Y. Pan, T. Xie, H. Kou, J. Li, Highly transparent $Tb_3Al_5O_{12}$ magneto-optical ceramics sintered from co-precipitated powders with sintering aids, Opt. Mater. 78 (2018) 370–374, https://doi.org/10.1016/j.optmat.2018.02.053.

[128] T. Zhou, L. Zhang, C. Shao, B. Sun, W. Bu, H. Yang, H. Chen, F.A. Selim, Q. Zhang, Sintering additives regulated Cr ion charge state in Cr doped YAG transparent ceramics, Ceram. Int. 44 (2018) 13820–13826, https://doi.org/10.1016/j.ceramint.2018.04.226.

[129] T.Y. Zhou, L. Zhang, H. Yang, X.B. Qiao, P. Liu, D.Y. Tang, J. Zhang, Effects of sintering aids on the transparency and conversion efficiency of Cr^{4+} ions in Cr: YAG transparent ceramics, J. Am. Ceram. Soc. 98 (2015) 2459–2464, https://doi.org/10.1111/jace.13616.

[130] V. V Balashov, Y.L. Kopylov, V.B. K, K. V Lopukhin, Vasylyna Shemet, Y.L. Zakharov, Fabrication of YAG:RE (RE = Yb, Nd, Cr) ceramics using divalent sintering aids, KnE Engineering 3 (2018) 106–112, https://doi.org/10.18502/keg.v3i6.2981.

[131] T. Zhou, L. Zhang, Z. Li, S. Wei, J. Wu, L. Wang, H. Yang, Z. Fu, H. Chen, C. Wong, Q. Zhang, Enhanced conversion efficiency of Cr^{4+} ion in Cr: YAG transparent ceramic by optimizing the annealing process and doping concentration, J. Alloys Compd. 703 (2017) 34–39, https://doi.org/10.1016/j.jallcom.2017.01.338.

[132] S. Liu, X. Feng, M. Nikl, L. Wu, Z. Zhou, J. Li, H. Kou, Y. Zeng, Y. Shi, Y. Pan, Fabrication and scintillation performance of nonstoichiometric LuAG:Ce ceramics, J. Am. Ceram. Soc. 98 (2014) 510–514, https://doi.org/10.1111/jace.13305.

[133] R. Gaume, Y. He, A. Markosyan, R.L. Byer, Effect of Si-induced defects on 1 μm absorption losses in laser-grade YAG ceramics, J. Appl. Phys. 111 (2012), 093104, https://doi.org/10.1063/1.4709756.

[134] P. Palmero, B. Bonelli, G. Fantozzi, G. Spina, G. Bonnefont, L. Montanaro, J. Chevalier, Surface and mechanical properties of transparent polycrystalline YAG fabricated by SPS, Mater. Res. Bull. 48 (2013) 2589–2597, https://doi.org/10.1016/j.materresbull.2013.03.003.

[135] A. Goldstein, A.I. Shames, A.J. Stevenson, Z. Cohen, M. Vulfson, Parasitic light absorption processes in transparent polycrystalline $MgAl_2O_4$ and YAG, J. Am. Ceram. Soc. 96 (2013) 3523–3529, https://doi.org/10.1111/jace.12525.

[136] A. Goldstein, M. Katz, R. Boulesteix, A.I. Shames, C. Coureau, J. Raethel, X. Mateos-Ferre, P. Loiko, Sources of parasitic features in the visible range of oxide transparent ceramics absorption spectra, J. Am. Ceram. Soc. 103 (2020) 4803–4821, https://doi.org/10.1111/jace.17182.

[137] L. Esposito, T. Epicier, M. Serantoni, A. Piancastelli, D. Alderighi, A. Pirri, G. Toci, M. Vannini, S. Anghel, G. Boulon, Integrated analysis of non-linear loss mechanisms in Yb:YAG ceramics for laser applications, J. Eur. Ceram. Soc. 32 (2012) 2273–2281, https://doi.org/10.1016/j.jeurceramsoc.2012.02.047.

[138] J. Hostaša, L. Esposito, A. Malchère, T. Epicier, A. Pirri, M. Vannini, G. Toci, E. Cavalli, A. Yoshikawa, M. Guzik, G. Alombert-Goget, Y. Guyot, G. Boulon, Polycrystalline Yb^{3+}-Er^{3+}-co-doped YAG: fabrication, TEM-EDX characterization,

spectroscopic properties, and comparison with the single crystal, J. Mater. Res. 29 (2014) 2288–2296, https://doi.org/10.1557/jmr.2014.206.
[139] W.Y. Sun, X.T. Li, L.T. Ma, T.S. Yen, Solubility of Si in YAG, J. Solid State Chem. 51 (1984) 315–320, https://doi.org/10.1016/0022-4596(84)90348-7.
[140] Y. Kuru, E.O. Savasir, S.Z. Nergiz, C. Oncel, M.A. Gulgun, Enhanced co-solubilities of Ca and Si in YAG ($Y_3Al_5O_{12}$), Phys. Status Solidi Curr. Top. Solid State Phys. 5 (2008) 3383–3386, https://doi.org/10.1002/pssc.200778902.
[141] G. Gilde, P. Patel, P. Patterson, D. Blodgett, D. Duncan, D. Hahn, Evaluation of hot pressing and hot isostatic pressing parameters on the optical properties of spinel, J. Am. Ceram. Soc. 88 (2005) 2747–2751, https://doi.org/10.1111/j.1551-2916.2005.00527.x.